Development of Yeast Expression System for Protein Crystallography

January 2009

Toshihiko KITAJIMA

Development of Yeast Expression System for Protein Crystallography

A Dissertation Submitted to
the Graduate School of Life and Environmental Science,
the University of Tsukuba
in Partial Fulfillment of the Requirements
for the Degree of Doctor of Philosophy in Science
(Doctoral Program in Functional Biosciences)

Toshihiko KITAJIMA

TABLE OF CONTENTS

TABLE OF CONTENTS ..... **i**

ABBREVIATIONS ..... **v**

ABSTRACT **1**

GENERAL INTRODUCTION **4**

Overview of glycosyltransferase 4

Production of selenomethionyl proteins in eukaryotic cells 6

The aim of this study 8

GENERAL METHODS **9**

Bacterial strain 9

Yeast strains 9

Culture conditions 9

Transformation of *E. coli* cells 10

Preparation of plasmid DNA from *E. coli* cells 10

Transformation of *S. cerevisiae* cells 11

Transformation of *P. pastoris* 11

Recovery of plasmid DNA from transformed yeast cells 12

Disruption of genes in yeast 13

SDS-polyacrylamide gel electrophoresis and immunoblots 13

CHAPTER 1

The novel activity of *Saccharomyces cerevisiae* α1,6-mannosyltransferase Och1p **15**

1-1. Summary **16**

1-2. Introduction **17**

1-3. Materials and Methods **20**

1-3-1. Plasmid construction and yeast transformation 20

1-3-2. Production and purification of recombinant Och1p 20

1-3-3. Mannosyltransferase assay 21

1-3-4. Preparation of crude enzyme containing wild-type or Och1 mutant protein 22

1-3-5. HPLC analysis of pyridylaminated oligosaccharides 22

1-3-6. Mannosidase treatment 23

1-4. Results **24**

1-4-1. Production and purification of recombinant Och1p 24

1-4-2. Substrate specificity 24

1-4-3. Properties of the recombinant α1,6-mannosyltransferase 26

1-4-4. Novel activity of Och1p 26

1-4-5. Structure of the novel product generated by Och1p 28

1-4-6. Effect of acceptor structure on the second mannose addition 29

1-5. Discussion **32**

CHAPTER 2

Use of novel selenomethionine-resistant yeast to produce selenomethionyl protein suitable for structural analysis **36**

2-1. Summary **37**

2-2. Introduction **38**

2-3. Materials and Methods **40**

2-3-1. Culture media and strains 40

2-3-2. Construction of expression vectors and strains 40
2-3-3. Immunoblots 41
2-3-4. Isolation of SeMet-resistant strains 41
2-3-5. Selenomethionyl HLY expression and purification 41
2-3-6. Analysis of SeMet content 42
2-3-7. Mass spectrometry 42
2-3-8. Crystallization, data collection and structure determination 43
2-4. Results 44
2-4-1. Isolation of SeMet-resistant mutants suitable for selenomethionyl protein expression 44
2-4-2. Evaluation of SeMet-resistant strain 45
2-4-3. Determination of selenomethionyl HLY structure 46
2-5. Discussion 47
CHAPTER 3
Characterization of novel selenomethionine-resistant mutant in *Saccharomyces cerevisiae* suitable for selenomethionyl protein production. 50
3-1. Summary 51
3-2. Introduction 52
3-3. Materials and Methods 54
3-3-1. Culture media and strains 54
3-2-2. Isolation of SeMet-resistant mutants in *S. cerevisiae* 54
3-3-3. Genetic analysis 54
3-3-4. Plasmid construction for *S. cerevisiae* 55
3-3-5. Microarray analysis 56

3-3-6. Identification of the genes that are responsible for SeMet resistance 56

3-3-7. Measurement of methionine uptake 57

3-4. Results 59

3-4-1. Isolation of SeMet-resistant mutants in *S. cerevisiae* 59

3-4-2. Global change of gene expression in SeMet-resistant mutants 59

3-4-3. Necessity of *de novo* synthesized methionine in SeMet-resistant mutants 60

3-4-4. Identification of genes responsible for SeMet resistance 61

3-4-5. External methionine uptake in *mup1* mutation 62

3-5. Discussion 64

GENERAL DISCUSSION 66

ACKNOWLEDGEMENTS 69

REFERENCES 71

FIGURES AND TABLES 82

ABBREVIATIONS

AdoMet	*S*-adenosylmethionine
ER	endoplasmic reticulum
E. coli	*Escherichia coli*
GDP-Man	guanosine diphosphate mannose
Glc	glucose
GlcNAc	*N*-acetylglucosamine
GO	gene ontology
HLY	human lysozyme
HPLC	high performance liquid chromatography
LiAc	lithium acetate
Man	mannose
MAD	multi-wavelength anomalous dispersion
M-Pol	mannan polymerase
OD	optical density
ORF	open reading frame
PA	2-aminopyridine
PVDF	polyvinylidene fluoride
SAD	single-wavelength anomalous dispersion
SDS-PAGE	SDS-polyacrylamide gel electrophoresis
SeMet	selenomethionine
UDP-Glc	uridine diphosphate glucose

ABSTRACT

Proteins can be covalently modified by the addition of oligosaccharide and further sugar residues can be added to form complex oligosaccharide structure. Glycosyltransferases are essential for formation of various kinds of oligosaccharides that serve as a wide range of biological function, such as protein activity, stability, quality control and cell-cell interaction. Thus, it is important to elucidate the molecular mechanism of glycosyltransferases for investigation of the physiological function of glycoproteins.

N-linked oligosaccharide is one of the major forms of protein glycosylation in eukaryotes. The α1,6-mannosyltransferase encoded by *OCH1* is a key enzyme for *N*-linked oligosaccharide modification in *Saccharomyces cerevisiae.* In order to characterize its enzymatic properties, the soluble form of the recombinant Och1p was expressed in the methylotrophic yeast *Pichia pastoris.* I revealed that the recombinant Och1p have a potential to transfer two molecules of mannose to $Man_9GlcNAc_2$-PA acceptors at high enzyme concentrations. I also found that Man-α1,2-Man-α1,3-Man, which is a common partial structure in acceptor oligosaccharides around the two molecules of mannose transferred, did not inhibit the first and second mannose transfer reactions. This result raised a possibility that Och1p strictly recognizes the tertiary structure of high mannose type oligosaccharides.

Second, in order to expedite investigation of molecular mechanism of glycosyltransferases including Och1p from the structural biological point of view, I attempted the development of selenomethionine-resistant mutant that can contribute to structure determination of proteins by X-ray crystallography. Selenomethionine

derivatives of proteins are useful to solve phase problem in protein crystallography, however selenomethionine is toxic compound for living cells, especially for eukaryotic cells. Accordingly, it has been difficult to prepare proteins with a high content of selenomethionine by eukaryotic expression system. To overcome this fundamental limitation, I reported the usefulness of the mutant that shows double-resistance to both SeMet and selenate. The mutant was able to produce human lysozyme containing selenomethionine at 65% occupancy. In addition, I demonstrated that the crystal structure of human lysozyme expressed by the mutant was successfully solved by using single-wavelength anomalous dispersion phasing method. As a result, I have succeeded in isolating selenomethionine-resistant mutant that is suitable for X-ray crystallography, serving as a host cell not only to produce selenomethionyl recombinant proteins in order to elucidate the substrate recognition mechanism of Och1p but also to prepare selenomethionine-labeled other glycosyltransferases that are generally difficult to be expressed in bacteria.

Next, to investigate the selenomethionine-resistant mechanism of the *Pichia* mutant I isolated above, I further isolated a mutant showing double-resistance to both SeMet and selenate in yeast *Saccharomyces cerevisiae* for genetic analysis. A genetic analysis allowed me to isolate a mutant allele of *MUP1* encoding high affinity methionine permease. The transcription of genes involved in methionine synthesis was slightly induced by the recessive mutation of *MUP1* (*mup1-100*). I also found that *mup1-100* cells had an ability enough to incorporate external methionine. These results indicate that *mup1* mutation causes overproduction of methionine up to the level that the cells can grow in the presence of selenate, and further suggest that the selenomethionine-resistant mutant I obtained will be useful to produce selenomethionyl

proteins to elucidate the crystal structure of eukaryotic proteins including glycosyltransferases.

GENERAL INTRODUCTION

Post-translational modification is a fundamental mechanism for the regulation of cellular physiology and function. Protein glycosylation is one of the well-known modifications in eukaryotic cells. It is estimated that about 50% of human proteins are modified by glycans (Kawasaki 2003). Protein glycosylation can be divided into two distinct classes based on binding modes of glycan to protein. One is *N*-linked glycosylation, in which a carbohydrate is bound to the asparagine residues in the sequence of Asn-X-Ser/The (X, any amino acids except for Pro) in the proteins with *N*-glycosidic bond. The other is *O*-linked glycosylation, in which a carbohydrate is bound to the Ser or Thr residues in the proteins with *O*-glycosidic bond. Theses glycosylated molecules play an important role of protein activity, protein stability, protein secretion, protein folding, correct targeting, interaction between proteins and cell-cell interaction in many living cells. The biosynthesis of theses carbohydrates includes a lot of reaction step by different glycosyltransferases.

Overview of glycosyltransferase

Glycosyltransferases (EC 2.4.x.y) catalyze the transfer of sugar moieties from activated donor molecules to specific acceptor molecules, forming glycosidic bonds. Depending on glycosyltransferases, the glycosylation reaction proceeds with either retention or inversion of the configuration of the anomeric carbon of donor sugar (Sinnott 1990). Genome sequencing has now revealed that more than 30,000 glycosyltransferase genes exist across all kingdoms. The enzymes have been classified into 91 families based on experimental characterization and amino acid sequence

similarity prediction (Cantarel *et al.* 2008), and these resources are available at Carbohydrate-Active Enzyme (CAZy) database (http://www.cazy.org).

X-ray crystallography can provide valuable information to understand the molecular mechanisms of glycosyltransferases. The first crystal structure of glycosyltransferase was reported in 1994 for bacteriophage T4 β-glucosyltransferase, which transfers glucose from UDP-Glc to phage-modified DNA (Vrielink *et al.* 1994). Two different superfamilies are now presented for glycosyltransferases, named GT-A and GT-B, which were first observed in SpsA and β-glucosyltransferase structures, respectively (Vrielink *et al.* 1994; Charnock and Davies 1999).

Some structural analyses provided a recognition mechanism accounting for specificity of donor substrate. A common feature of GT-A enzymes is the presence of Asp-X-Asp (DXD) motif, and also the requirement for a divalent cation for enzymatic activity (Breton *et al.* 1998; Breton and Imberty 1999). The DXD motif interacts with the phosphate groups of sugar nucleotide through the coordination of divalent cation, typically Mn^{2+}. Differences are observed in the function of the motif in retaining and inverting enzymes. In retaining enzymes, the two aspartate residues can interact with cation, whereas only the last aspartate interacts with cation in inverting enzyme (Persson *et al.* 2001; Tarbouriech *et al.* 2001). In both cases, the variable amino acid between aspartate residues of the DXD motif is involved in ribose binding. On the other hand, the GT-B fold consists of two separate domains separated by a cleft that is catalytic site. The GT-B glycosyltransferases do not possess a DXD motif, although divalent cations are required for full activity of GT-B enzymes.

Despite a donor specificity of glycosyltransferases have been elucidated, little is known about a molecular mechanism for the recognition of acceptor substrate. One

reason is that the crystal structures that have been described for glycosyltransferases are few to find out common properties although the variety of acceptor substrates is abundant more than donor substrate. Until now, 206 crystal structures are described for proteins corresponding to only 26 glycosyltransferase families.

Difficulties with high-level expression and crystallization hamper the determination of crystal structure for glycosyltransferases. Most of the glycosylation reactions that generate a diversity of oligosaccharide structures of eukaryotic cells occur in the endoplasmic reticulum (ER) or the Golgi apparatus. Thus, glycosyltransferases involved in protein glycosylation are difficult to be overproduced in bacterial expression system, which is most generally used to prepare recombinant proteins. Now, various kinds of eukaryotic expression system are available. Yeast is one of attractive hosts for producing eukaryotic proteins among them because yeast expression system includes simple culture conditions and straightforward scale-up to fermentation. Even if the proteins are successfully prepared by the eukaryotic expression system, problems, such as phase determination, remain to be addressed.

Production of selenomethionyl proteins in eukaryotic cells

One way to solve phase problem is a single-wavelength anomalous dispersion (SAD) or multi-wavelength anomalous dispersion (MAD) phasing of crystals of proteins whose methionine residues are replaced with selenomethionine (SeMet) (Hendrickson *et al.* 1990; Rice *et al.* 2000). Recent advance in structural biology strongly depends on SAD or MAD phasing methods because SeMet derivatives of proteins are easily produced in *Escherichia coli*. In contrast, it is more difficult to replace methionine with SeMet in eukaryotic cells other than *E. coli* cells because

SeMet is toxic compound for living cells (Schrauzer 2003). However, the toxic mechanism of SeMet is still unknown.

Many studies have reported the production of SeMet derivatives in eukaryotic cells, such as Chinese hamster ovary cells (Lustbader *et al.* 1995; Davis *et al.* 2001), HEK293 cells (Barton *et al.* 2006), insect cells (Cronin *et al.* 2007), *Saccharomyces cerevisiae* (Bushnell *et al.* 2001; Laurila *et al.* 2005) and *Pichia pastoris* (Larsson *et al.* 2002; Xu *et al.* 2002). Most of the reports presented methodology for SeMet substitution in each host; however, SeMet toxicity on recombinant protein expression was rarely studied. Unlike higher eukaryotic cells, yeasts have the potential to minimize or eliminate SeMet toxicity through SeMet-resistant mutants.

There are several reports on the SeMet-resistant mutants in budding yeast *Saccharomyces cerevisiae.* In 1970s, *sam1* and *sam2* mutant cells that were resistant to both SeMet and ethionine, which is another methionine analogue, were isolated by a spontaneous mutation (Cherest *et al.* 1973; Cherest and Surdin-Kerjan 1981). Biochemical analysis demonstrated that these mutations led to a considerable increase in endogenous cellular methionine pool (Cherest *et al.* 1973). Most recent works demonstrated that *sam1*Δ *sam2*Δ cells and *cys3*Δ cells are resistant to SeMet and able to produce SeMet-labeled protein with >90% occupancy (Malkowski *et al.* 2007; Bockhorn *et al.* 2008), although these mutants require *S*-adenosylmethionine (AdoMet) or cysteine as a supplement, which is an expensive and unstable compound. To produce large amounts of SeMet-derivatives of eukaryotic proteins in yeasts, it is necessary to develop a new SeMet-resistant mutant that can efficiently incorporate SeMet into proteins and grow without supplementation of sulfur amino acids.

The aim of this study

In this situation, I reported the characterization of acceptor specificity of *S. cerevisiae* glycosyltransferase Och1p that is responsible for the initiation of the *N*-linked oligosaccharide elaboration in the Golgi apparatus in Chapter 1. To develop a useful tool for the investigation of substrate recognition mechanism of glycosyltransferases from the point of view of structural biology, and then I attempted the use of novel SeMet-resistant mutant that can contribute to X-ray structural analysis in Chapter 2. Finally, I reported the functional characterization of the SeMet-resistant mutant in Chapter 3.

GENERAL METHODS

Bacterial strain

For standard DNA propagation the strain DH5α (F^-, Φ80d *lacZ*ΔM15, Δ(*lacZYA-argF*)U169, *deoR*, *recA*1, *endA*1, *hsdR*17(r_K^- m_K^+), *phoA*, *supE*44, λ^-, *thi*-1, *gyrA*96, *relA*1) was used.

Yeast strains

Yeast strains used in this study are listed in Table 1. W303-1A (*MAT***a** *ade2-1 his3-11 leu2-3,-112 trp1-1 ura3-1 can1-100*) was used as wild-type cells of budding yeast *S. cerevisiae* (Sutton *et al.* 1991). Methylotrophic yeast *P. pastoris* SMD1168 (*pep4 his4*) and GS115 (*his4*) were used for the production of recombinant proteins (Invitrogen, Carlsbad, CA, USA).

Culture conditions

E. coli strains were grown in LB medium (1% [w/v] Bacto-Tryptone (Difco, Detroit, Michigan, USA), 0.5% [w/v] Bacto-Yeast Extract (Difco), 0.5% [w/v] NaCl, pH 7.0) at 37˚C.

Yeast strains were cultivated in YPD medium (2% [w/v] glucose, 2% [w/v] Bacto-Peptone (Difco) and 1% [w/v] Bacto-Yeast Extract). YPAD medium, which was YPD medium containing 0.01% (w/v) adenine sulfate, was used for adenine auxotrophic strains. BMGY medium (100 mM potassium phosphate buffer [pH 6.0],

1% [w/v] Bacto-Yeast Extract, 2% [w/v] Bacto-Peptone, 1.34% [w/v] Bacto-Yeast Nitrogen Base w/o amino acids (Difco), 400 μg/ml biotin, 1% [w/v] glycerol) was used for *P. pastoris* cultivation. For auxotrophic selection, Synthetic Dextrose (SD) medium (2% [w/v] glucose, 0.67% [w/v] Bacto-Yeast Nitrogen Base w/o amino acids) was also used. SD was supplemented with the amino acids and nucleic acid bases required to complement the auxotrophic requirements of each strain. For tryptophan and uracil auxotrophic selection, SDCA medium (SD medium containing 0.5% [w/v] Bacto-Casamino Acids (Difco) and 0.01% [w/v] adenine sulfate) was used. Yeast strains were cultivated at 30˚C.

Transformation of *E. coli* cells

Transformation of *E. coli* cells was done according to the method of Hanahan (Hanahan 1983). One hundred μl of competent cells (purchased from Toyobo, Osaka, Japan) was gradually thawed and mixed gently with 5 μl of DNA solution. After incubation for 30 min on ice, cells were heat-shocked at 42˚C for 45 sec. Immediately 900 μl of SOC medium (2% [w/v] Bacto-Tryptone, 0.5% [w/v] Bacto-Yeast Extract, 10 mM NaCl, 2.5 mM KCl, 10 mM $MgSO_4$, 10 mM $MgCl_2$, 20 mM glucose) was added. After incubation for 1 h at 37˚C in water bath, the culture medium was spread onto LB-Amp plate (LB medium containing 100 μg/ml ampicillin and 1.5% [w/v] agar) or LB-Zeo (LB-medium containing 25 μg/ml Zeocin and 1.5% [w/v] agar), allowed to cultivate overnight at 37˚C.

Preparation of plasmid DNA from *E. coli* cells

E. coli cells which contain plasmid DNA were cultured overnight in 5 ml of

LB-Amp medium (LB medium containing 100 μg/ml ampicillin) or LB-Zeo (LB-medium containing 25 μg/ml Zeocin). Plasmid DNA was extracted by QIAprep Spin Miniprep Kit (Qiagen, Hilden, Germany).

Transformation of *S. cerevisiae* cells

Transformation of *S. cerevisiae* cells was done according to the method of Gietz (Gietz *et al.* 1995). *S. cerevisiae* cells were incubated in 2 ml YPAD of medium overnight at 30˚C with shaking. The precultured cells were inoculated to 50 ml of YPAD (~ 0.3 OD_{600}). The cells were grown for 5 h. Cells were harvested in the sterile plastic tubes at 3000 × *g* for 5 min and the pellet was collected. Then cells were suspended in 20 ml of sterile water and centrifuged again. The cell pellet was resuspended in 1 ml of 100 mM LiAc and transferred to a 1.5 ml microtube. The suspension was centrifuged at top speed for 15 sec and the supernatant was removed with a micropipette. The cells were resuspended in 100 mM LiAc for a final volume of approximately 500 μl. Then 50 μl of the competent cells was added to the transformation mixture (240 μl of 50% [w/v] PEG 4000, 36 μl of 1 M LiAc, 12.5 μl of 4 mg/ml carrier DNA, 57.5 μl of sterile water and 5 μl of plasmid DNA) and vortexed well. The suspension was incubated at 30˚C for 30 min and then heat-shocked at 42˚C for 20 min. The mixture was centrifuged and the supernatant was removed. The cell pellet was resuspended in 200 μl of sterile water and spread on a selective medium plate.

Transformation of *P. pastoris*

Transformation of *P. pastoris* cells was done according to the manufacturer's

protocol (Invitrogen). For electroporation method, *P. pastoris* cells were incubated overnight at 30˚C in 5 ml of YPD medium. One hundred μl of the overnight culture was inoculated to 500 ml YPD and grown overnight again to an OD_{600} = 1.3–1.5. Cells were harvested in the sterile plastic tubes at 1500 × *g* for 5 min at 4˚C. Then cells were washed twice with sterile ice-cold water. The cells were suspended in 20 ml of ice-cold 1 M sorbitol and centrifuged. The cell pellet was resuspended in ice-cold 1 M sorbitol for a final volume of approximately 1.5 ml. Then 80 μl of cell suspension was mixed with 10 μl of plasmid DNA linearized by an appropriate restriction enzyme and transferred to ice-cold electroporation cuvette. After incubation on ice for 5min, the cells were pulsed at 2.0 kV on MicroPulser (Bio-Rad, Hercules, CA, USA). Then 1 ml of ice-cold 1M sorbitol was added to the cuvette and the suspension was transferred to sterile 15 ml tube. After incubation at 30˚C for 2 h, the cells were spread on a selective medium plate. Alternatively, LiCl method was also used for *P. pastoris* transformation. The procedure for *P. pastoris* was identical to that for *S. cerevisiae*, but LiCl reagent was used instead of LiAc reagent.

Recovery of plasmid DNA from transformed yeast cells

Yeast cells previously grown in 3 ml of selective medium were collected by centrifugation. Then 300 μl of yeast breaking buffer (10 mM Tris-HCl [pH 8.0], 0.1 M NaCl, 1 mM EDTA, 2% [v/v] Triton X-100, 1% [w/v] SDS) was added. Acid washed glass beads (0.5 mm in diameter; Sigma, St. Louis, MO, USA) were filled into the microtube up to the meniscus. Three hundred μl of phenol/chloroform was added and vortexed for 5 min. The aqueous phase was transferred into a clean tube containing 200 μl of chloroform and stirred. The aqueous phase was recovered and mixed with 500 μl

of ethanol and 20 μl of 3 M sodium acetate (pH 5.2). DNA was precipitated by centrifugation, rinsed with cold 70% (v/v) ethanol and resuspended in 10 μl of TE buffer (10 mM Tris-HCl [pH 8.0], 0.1 mM EDTA). About 2 μl of the DNA solution was used to transform *E. coli* cells.

Disruption of genes in yeast

Disruption of genes in yeast was performed with one step gene disruption method as described by Longtine *et al.* (1998). PCR was performed using pFA6a-KanMX6 and pFA6a-His3MX plasmids (Longtine *et al.* 1998) as templates. Appropriate forward target gene-specific primer with 5'-CGGATCCCCGGGTTAATTAA-3' at the 3' end and reverse target gene-specific primer with 5'-GAATTCGAGCTCGTTTAAAC-3' at the 3' end were used. The PCR product was introduced to yeast host cells. The transformants were selected with appropriate auxotrophy, and checked the insertion site with yeast colony PCR using one primer that annealed within the transformation module and the second primer that annealed to the target gene locus outside the region altered.

SDS-polyacrylamide gel electrophoresis and immunoblots

SDS-polyacrylamide gel electrophoresis (SDS-PAGE) was conducted as follows. An equal volume of 2 × loading buffer (0.1 M Tris-HCl [pH 6.8], 0.2 M DTT, 4% [w/v] SDS, 0.2% [w/v] bromo phenol blue, 20% [v/v] glycerol) was added to samples. The samples were denatured at 95˚C for 5 min and run on SDS-polyacrylamide gels as described by Laemmli (1970). After electrophoresis, the gels were stained with Gel Code Blue Stain Reagent (PIERCE, Rockford, IL, USA) to

visualize proteins.

For immunoblotting, the proteins on the polyacrylamide gel were transferred to polyvinylidene fluoride (PVDF) membrane with ATTO transfer system (ATTO, Tokyo, Japan) with constant current (2 mA/cm^2 membrane) for 1 h. The PVDF membrane was incubated in blocking buffer (TBS-T (25 mM Tris-HCl [pH7.4], 137 mM NaCl, 2.7 mM KCl, 0.1% [v/v] Tween-20) containing 5% [w/v] skim milk) for 1 h. Primary antibody was diluted by blocking buffer and PVDF membrane was incubated in diluted primary antibody solution for 1 h at room temperature or overnight at 4˚C. After the incubation, the PVDF membrane was washed two times for 10 min with TBS-T. Secondary antibody was diluted by blocking buffer and the membrane was incubated in secondary antibody solution for 1 h at room temperature. After washing two times for 10 min with TBS-T, the membrane was incubated with ECL-plus or CDP-Star reagents (GE Healthcare, Buckinghamshire, United Kingdom) for 5 min. Then the chemiluminescence was analyzed by LAS 1000 plus (Fuji Film, Tokyo, Japan).

CHAPTER 1

The novel activity of *Saccharomyces cerevisiae* α1,6-mannosyltransferase Och1p

1-1. Summary

In yeast, the *N*-linked oligosaccharide modification in the Golgi apparatus is initiated by α1,6-mannosyltransferase (encoded by the *OCH1* gene) with the addition of mannose to the $Man_8GlcNAc_2$ or $Man_9GlcNAc_2$ endoplasmic reticulum intermediates. In order to characterize its enzymatic properties, the soluble form of the recombinant Och1p was expressed in the methylotrophic yeast *Pichia pastoris* as a secreted protein, after truncation of its transmembrane region and fusion with myc and histidine tags at the C-terminus, and purified using a metal chelating column. The enzymatic assay was performed using various kinds of pyridylaminated (PA) sugar chains as acceptor, and the products were separated by high performance liquid chromatography (HPLC). The recombinant Och1p efficiently transferred a mannose to $Man_8GlcNAc_2$-PA and $Man_9GlcNAc_2$-PA acceptors, while $Man_5GlcNAc_2$-PA, which completely lacks α1,2-linked mannose residues, was not used as an acceptor. At high enzyme concentrations, a novel product was detected by HPLC. Analysis of the product revealed that a second mannose was attached at the 6-*O*-position of α1,3-linked mannose branching from the α1,6-linked mannose that is attached to β1,4-linked mannose of $Man_{10}GlcNAc_2$-PA produced by the original activity of Och1p. Our results indicate that Och1p has the potential to transfer two mannoses from GDP-mannose, and strictly recognizes the overall structure of high mannose type oligosaccharide.

1-2. Introduction

In eukaryotes, *N*-linked protein glycosylation begins in the endoplasmic reticulum (ER) with the transfer of the lipid-linked $Glc_3Man_9GlcNAc_2$ precursor to nascent proteins, and then the sugar chain moieties are rapidly trimmed by removal of the three glucose residues and, in some cases, a specific α1,2-linked mannose residue to generate homogenous $Man_8GlcNAc_2$ intermediates (Helenius and Aebi 2001). The early stages of *N*-linked oligosaccharide synthesis in the ER are common in yeast and mammals. However, the final *N*-linked oligosaccharide structure generated in the Golgi apparatus varies among species. Budding yeast, *Saccharomyces cerevisiae*, do not further trim the $Man_8GlcNAc_2$ ER intermediate, whereas mammalian cells usually do (Byrd *et al.* 1982). *S. cerevisiae* has two major forms of *N*-glycan elongated from $Man_8GlcNAc_2$ ER intermediate with a different extent of mannose addition (Gemmill and Trimble 1999). Most glycoproteins localized in internal organelles have short oligosaccharides (core type), in which a few mannose residues are added to the $Man_8GlcNAc_2$ intermediate, while many of the glycoproteins localized in the cell wall and periplasm have a large mannan structure (outer chain) of up to 200 mannose residues (Dean 1999). In both cases, modification in the Golgi is initiated by α1,6-mannosyltransferase (Och1p), which transfers an α1,6-mannose to the α1,3-linked mannose that is attached to the β1,4-mannose of the $Man_8GlcNAc_2$ (Nakayama *et al.* 1992; Nakanishi-Shindo *et al.* 1993). The attached mannose acts as a scaffolding residue that is required for further elongation on the α1,6-mannose backbone by two complexes called mannan polymerase (M-Pol) I and II (Jungmann and Munro 1998;

Jungmann *et al.* 1999). After elongation, Mnn2p and Mnn5p add the first and second mannose with α1,2-linkage to the backbone (Rayner and Munro 1998), and the terminal mannose is added by Mnn1p with α1,3-linkage (Yip *et al.* 1994; Wiggins and Munro 1998).

Although yeast has various kinds of glycosyltransferases involved in glycoprotein biosynthesis, as described above, only a few glycosyltransferases have been characterized enzymatically and biochemically. Some α1,2-mannosyltransferases such as Kre2p/Mnt1p and Ktr1p have been exceptionally well characterized as recombinant proteins (Romero *et al.* 1997; Thomson *et al.* 2000). Romero *et al.* (1997) demonstrated that soluble enzyme produced in *P. pastoris* showed that Kre2p/Mnt1p was involved in both *N*-linked outer chain and *O*-linked oligosaccharide synthesis. Moreover, the three-dimensional structure of Kre2p/Mnt1p led to an understanding of catalytic mechanism of α1,2-mannosyltransferase (Lobsanov *et al.* 2004). Regarding α1,6-mannosyltransferase, only Och1p has been characterized so far. The in vivo function of Och1p was confirmed by the absence of the outer chain in *och1*Δ cells (Nakanishi-Shindo *et al.* 1993), and the enzymatic reactions were characterized by using Och1p-overproducing cells (Nakayama *et al.* 1997). Substrate-specificity studies demonstrated that Och1p recognized not only the residue to which the α1,6-mannose is added but also the several surrounding residues, but little is known about the enzymatic properties (Nakayama *et al.* 1997).

The enzymes responsible for the initiation of the outer chain were found in other fungi, such as *Schizosaccharomyces pombe* and *Yarrowia lipolytica*, as well as *S. cerevisiae* (Yoko-o *et al.* 2001; Barnay-Verdier *et al.* 2004). Further characterization is necessary to understand the high-mannose type oligosaccharide recognition mechanism

and to develop new antifungal agents that specifically inhibit the enzymatic reaction, because this reaction is unique to fungi and does not occur in mammals. In this study, I produced recombinant Och1p lacking the N-terminal transmembrane domain as a secreted form by using the *P. pastoris* expression system and purified it from the culture supernatant. Here, I report the analysis of the reaction products, and conclude that Och1p has the potential to transfer two mannose residues to $Man_9GlcNAc_2$ acceptor.

1-3. Materials and Methods

1-3-1. Plasmid construction and yeast transformation

The *OCH1* gene lacking the sequence encoding the putative transmembrane region was amplified by PCR with two primers, OCH1-FW (5'-CTCGAGAAAAGACACTTGTCAAACAAAAGGCTGCTT-3') and OCH1-RV (5'-TCTAGACGTTTATGACCTGCATTTTTATCAGCA-3'), and *S. cerevisiae* YPH500 genome DNA as a template. The amplified fragment was digested with *Xba*I and *Xho*I, and then purified. The purified fragment was ligated into the corresponding sites of pPICZαA to generate pPICZαA-ScOCH1, and sequenced for confirmation. Transformation of *P. pastoris* GS115 and selection were conducted according to the manufacturer's protocol. The expression vector (pPICZαA-ScOCH1) was linearized by *Pme*I and used to transform *P. pastoris* by the electroporation method. Direct PCR of transformed colonies using two primers, 5'AOX1 and 3'AOX1 (Invitrogen), confirmed the integration of the expression cassette.

1-3-2. Production and purification of recombinant Och1p

Transformed *P. pastoris* cells were inoculated into 100 ml of BMGY. After overnight cultivation at 30˚C, an inoculum was added to 6 L of BMGY media in an 8-L jar-fermentor. To maintain the dissolved oxygen at 10% of saturation level, the flow rate of air and agitation were controlled automatically using a process controller system (EPC-2000; EYELA, Tokyo, Japan). The pH of the medium was maintained at 6.0 with ammonium hydroxide. Cultivation was continued at 30˚C until the glycerol, as a carbon source, was completely consumed. After depletion of glycerol, the temperature was

shifted to 24˚C and methanol feeding was started to induce the production of recombinant Och1p. The methanol was supplied continuously with a peristaltic pump at 10–15 ml/h. During the methanol feeding, 0–0.5 L/min of pure oxygen was supplied in addition to air. After two days of induction, the culture supernatant was collected by centrifugation, then concentrated and desalted by ultrafiltration (MWCO 10000; Microza UF, Asahikasei, Tokyo, Japan).

The concentrated supernatant was applied to TALON Metal Affinity Resin (Clontech, CA, USA), equilibrated with 50 mM sodium phosphate (pH7.0) containing 300 mM NaCl, and washed with 50 mM sodium phosphate (pH7.0) containing 300 mM NaCl and 18 mM imidazole. Elution was performed with 50 mM sodium phosphate (pH7.0) containing 300 mM NaCl and 99 mM imidazole. The eluate was concentrated and loaded onto a Superdex 200 10/300 GL column (GE Healthcare). The chromatography was carried out with 50 mM Tris-HCl (pH8.0) containing 150 mM NaCl, and fractions containing recombinant Och1p were collected. The purified enzyme was concentrated to 1.5 mg/ml and stored at -80˚C.

1-3-3. Mannosyltransferase assay

Standard reaction mixtures contained 50 mM Tris-HCl (pH7.5), 10 mM $MnCl_2$, 1 mM GDP-mannose (Sigma), 2 μM pyridylaminated oligosaccharide acceptor (TaKara, Shiga, Japan) and Och1p in a total volume of 10 μl. Before the measurement of Och1p activity, the stored protein was diluted to an appropriate concentration with 50 mM Tris-HCl (pH7.5) (the protein concentration is indicated in the figure legends). Unless stated otherwise, incubation was done at 30˚C for 5 min and terminated by adding 30 μl of 50 mM EDTA. The reaction mixtures were then subjected to HPLC

analysis.

1-3-4. Preparation of crude enzyme containing wild-type or Och1 mutant protein

To construct the expression vector for mutant Och1p (pPICZαA-D187A), which is substituted the Asp residue at the position of 187 with Ala, I used QuickChange II Site-directed Mutagenesis Kit (Stratagene, La Jolla, CA, USA) by using two mutagenic primers, which were D187A-FW (5'-CAAGAGGTGGTATTTACTCAGCTATGGATACTATGCTTTTGAA-3') and D187A-RV (5'-TTCAAAAGCATAGTATCCATAGCTGAGTAAATACCACCTCTTG-3'), and the pPICZαA-ScOCH1 as a template. The both D187A mutant and wild-type proteins were expressed as mentioned above. After the culture supernatants were concentrated about 300-fold, the amount of secreted Och1p were estimated by the immunoblotting using antibody against Och1p (Nakayama *et al.* 1992). The same amount of Och1p was used for the mannosyltransferase assay. The reaction mixtures were subject to HPLC analysis.

1-3-5. HPLC analysis of pyridylaminated oligosaccharides

Pyridylaminated oligosaccharides were separated by size fractionation HPLC. All samples were boiled and filtrated (Ultrafree-MC; Millipore, Billerica, MA, USA) prior to analysis to remove proteins and other insoluble materials. Elution was carried out at a flow rate of 1.0 ml/min with solvent A (100% acetonitrile) and solvent B (0.2 M acetic acid/triethylamine [pH 7.0]). Three different methods were used. In method 1, the samples were separated using TSK-gel Amide-80 (4.6 × 250 mm; Tosoh, Tokyo, Japan)

with a linear gradient from 38% to 50% solvent B for 30 min. In method 2, the samples were separated using Asahipak NH2P-50 (4.6 × 250 mm; Showadenko, Tokyo, Japan) with a linear gradient from 25% to 50% solvent B for 60 min. In method 3, the samples were separated using Asahipak NH2P-50 with a linear gradient from 37.5% to 50% solvent B for 30 min. Eluted pyridylaminated oligosaccharides were monitored by fluorescence (315 nm for excitation, 380 nm for emission) and collected individually at the detector outlet.

1-3-6. Mannosidase treatment

The oligosaccharides were digested with α1,2-mannosidase (Seikagaku Corp., Tokyo, Japan) or α1,6-mannosidase (New England Biolabs, Beverly, MA, USA) according to the manufacturer's protocols. The reaction mixtures were boiled and filtrated prior to analysis, as described above.

1-4. Results

1-4-1. Production and purification of recombinant Och1p

Och1p is a type-II transmembrane protein that is anchored to the Golgi apparatus at its N-terminus and has an α1,6-mannosyltransferase activity (Nakayama *et al.* 1992). To characterize its enzymatic properties, a soluble form of recombinant Och1p was produced in *P. pastoris* as a secreted protein. For this purpose, the DNA sequence encoding the catalytic domain of Och1p was cloned into the pPICZαA expression vector. In this case, the N-terminal region of Och1p was replaced with the α-factor prepro sequence, which facilitates the secretion of protein into the medium (Cregg *et al.* 1993; Scorer *et al.* 1993), and this construct was further fused with myc and His_6-tag at the C-terminus. The resulting construct, which is designated pPICZαA-ScOCH1, encoded residues 31–480 of native Och1p (see Figure 1A).

The recombinant Och1p was expressed in *P. pastoris* GS115 strain that was transformed with pPICZαA-ScOCH1 as described in Materials and Methods. The expressed protein was purified from the culture medium on a metal chelating affinity column. To eliminate trace contaminants, gel filtration chromatography was performed. Finally, I obtained purified Och1p giving a single band in SDS-PAGE with a yield of approximately 2 mg per 6 L of culture supernatant (Figure 1B).

1-4-2. Substrate specificity

To examine the acceptor specificity of recombinant Och1p, pyridylaminated derivatives of several high mannose type oligosaccharides (shown in Figure 2) were

collected and used as acceptors. As shown in Table 2, M8A was a good acceptor for Och1p; however, the lack of α1,2-linked mannoses in acceptors caused a decrease in mannosyltransferase activities. Interestingly, neither M5A, which completely lacks α1,2-mannose, nor M6C, in which the α1,2-mannose is attached at the No. 8 position (middle arm) of M5A (Figure 2), was recognized as an acceptor (Table 2). The mannosyltransferase activities were recovered up to 15% of control toward the M6B and M7B acceptors, in which one or two α1,2-linked mannose residues are attached at the No. 6 and 9 positions (lower arm) of M5A, respectively (Table 2 and Figure 2). The enzymatic reaction occurred more efficiently with M7A than with M7B (Table 2), which have one α1,2-linked mannose residue at the No. 7 position (upper arm) or No. 9 position (lower arm), respectively (Figure 2). However, the relative activity toward M7D, which has α1,2-mannose at the No. 8 position (middle arm), was not different from that toward M6B (Table 2). These results indicated that an α1,2-mannose residue at the upper arm was most important for the substrate recognition, although Och1p transfers a mannose residue at the No. 3 position. Moreover, α1,2-linked mannose at the upper arm was more important for Och1p than the same moiety at the lower arm, while that at the middle arm did not participate in the mannose addition.

In addition, these substrate recognition patterns were very similar to those reported previously, which were established by the use of microsomal fractions prepared from cells overexpressing the *OCH1* gene as an enzyme source (Yoko-o *et al.* 2001), suggesting that the absence of the transmembrane region and the fusion with myc-His_6 tag at the C-terminus did not affect the enzymatic activity of Och1p.

1-4-3. Properties of the recombinant α1,6-mannosyltransferase

The effects of several divalent cations, Mn^{2+}, Mg^{2+}, Ca^{2+}, Co^{2+}, Ni^{2+}, Cu^{2+}, Zn^{2+} and Cd^{2+}, on the mannosyltransferase activity were studied. As shown in Table 3, the enzymatic activity was not observed without metal ion. Only the addition of Mn^{2+} restored the activity, and the other cations showed no significant effects on the enzymatic activity. The absolute requirement of this enzyme for Mn^{2+} was similar to that previously reported for α1,2-mannosyltransferases (Kre2p/Mnt1p and Ktr1p) of *S. cerevisiae* (Romero *et al.* 1997). I also analyzed the pH profile of Och1p. The recombinant Och1p in Tris-malate buffer exhibited above 80% of maximum activity between pH 6.5 and 8.5, with a define peak at pH 7.5 (data not shown). It is known that the secretory pathway becomes increasingly acidic from the ER to the Golgi (Wu *et al.* 2001). It is likely that Och1p, which is localized mainly in the *cis*-Golgi compartment (Gaynor *et al.* 1994), is sufficiently active to initiate the outer chain elongation *in vivo.* In addition, a similar result (maximum activity at pH 7.0 and 95 % of maximum activity at pH 6.5) was reported for the recombinant Ktr1p, which is also localized mainly in the *cis*-Golgi and is capable of participating in both *N*-glycan and *O*-glycan biosynthesis (Romero *et al.* 1997).

1-4-4. Novel activity of Och1p

The reaction products generated from pyridylaminated acceptor oligosaccharides by the recombinant Och1p were analyzed by HPLC. When the enzymatic reaction was performed with the $Man_9GlcNAc_2$-PA acceptor (M9A shown in Figure 2) and 150 μg/ml of Och1p, $Man_{10}GlcNAc_2$-PA and an unexpected product were observed (peak 3 in Figure 3A). Since Och1p is responsible for the addition of a

mannose to the lower arm (No. 3 position of M9A in Figure 2) with α1,6-linkage, the substrate (peak 1) was converted to $Man_{10}GlcNAc_2$-PA (peak 2) within 10 min, and then the novel product (peak 3) newly appeared at 10 min and increased with the reaction period. To confirm that peak 3 was a derivative of the M9A acceptor, all peaks were collected and analyzed by MALDI-TOF mass spectrometry (Figure 3B). The MS spectra of peaks 1 and 2 showed prominent peaks at *m/z* 1962 and 2124, which corresponded to the *m/z* values of M9A and $Man_{10}GlcNAc_2$-PA, respectively. The MS analysis of peak 3 gave an ion peak at *m/z* 2286, which was interpreted as $[M+H]^+$. This result strongly suggests that peak 3 represents pyridylaminated oligosaccharide in which one molecule of hexose has been added to $Man_{10}GlcNAc_2$-PA. This additional hexose is probably a mannose residue because the recombinant Och1p was incubated in the presence of GDP-mannose (>98% purity) as a donor.

Because the enzyme reaction was performed under high concentration of Och1p, it theoretically remains the possibility that the novel activity was due to a trace amount of contaminants, such as glycosyltransferases from the *P. pastoris* host cells, although the enzyme was purified by metal chelating affinity column. To exclude this possibility, I expressed Och1 mutant protein lacking its activity and measured the novel mannosyltransferase activity by using the culture medium as an enzyme source. Glycosyltransferases generally contain an Asp-X-Asp sequence (DXD motif) in its active site that is necessary for catalytic activity, and Och1p also possesses the motif at the position of 187–189 (Wiggins and Munro 1998). I constructed the expression vector for Och1 mutant protein (D187A), in which the Asp residue at 187 was substituted with Ala. Predictably, D187A mutant did not have any mannosyltransferase activity. Because the novel activity was observed only under high concentration of purified Och1p, the

culture supernatant should be concentrated. The wild-type and D187A were expressed and concentrated by the same ultrafiltration procedures, respectively. Immunoblotting using anti-Och1p antibody (Nakayama *et al.* 1992) revealed that the concentration of D187A mutant protein in the crude enzyme was about 4-fold lower than that of wild-type, which may be due to the difference in the expression level or stability of secreted protein. For this reason, the crude enzyme containing wild-type was diluted 4-fold to match the D187A mutant protein concentration in the crude enzymes. Since the concentration fold of D187A was higher than that of wild-type, the contaminants, if present, should be more abundant in crude enzyme containing D187A than wild-type Och1p. Since it was thought that the contaminants might have a catalytic activity only toward $Man_{10}GlcNAc_2$-PA, where the first mannose was added to $Man_9GlcNAc_2$-PA, I purified $Man_{10}GlcNAc_2$-PA and used as an acceptor, which was synthesized from $Man_9GlcNAc_2$-PA by using purified Och1p. The enzyme assay revealed that the crude enzyme containing wild-type showed the novel mannosyltransferase activity towards $Man_{10}GlcNAc_2$-PA, whereas the D187A mutant did not show any activity under the same conditions. Moreover, the activity of D187A mutant was not detected by the increase of the reaction period, although the 8-fold diluted crude enzyme containing wild-type Och1p still showed mannosyltransferase activity (Figure 3C). These results indicated that the addition of the second mannose residue was not due to the contamination from the expression host, demonstrating that Och1p had the catalytic potential to transfer two molecules of mannose to M9A acceptor.

1-4-5. Structure of the novel product generated by Och1p

To confirm the position of incorporation of the novel second mannose,

$Man_{10}GlcNAc_2$-PA and the novel product (M10 and M11 in Figure 4A, respectively) were collected and digested with two kinds of mannosidases and analyzed by size-fractionation HPLC. The novel product was not digested with the α1,6-mannosidase (derived from *Xanthomonas manihotis*, data not shown), indicating that the second mannose was not attached to the non-reducing terminus with α1,6-linkage, because the α1,6-mannosidase used in this study is known to catalyze the hydrolysis of a terminal Man-α1,6-linkage that is linked to a non-branched sugar. When digested with the recombinant α1,2-mannosidase (derived from *Aspergillus saitoi*), M10 and M11 were shifted to $Man_6GlcNAc_2$-PA and $Man_7GlcNAc_2$-PA, respectively (M6 and M7 in Figure 4B, respectively). This result indicated that the second mannose was not attached to any of the four α1,2-linked mannoses that existed on the M9A acceptor (Figure 2). Next, the products of α1,2-mannosidase treatment were further digested with the above α1,6-mannosidase. Both the M6 and M7 peaks in Figure 4B were shifted to $Man_5GlcNAc_2$-PA (M5 in Figure 4C). This result indicated that the second mannose is attached with α1,6-linkage to either the α1,6-linked or the α1,3-linked mannose that is attached to α1,6-linked mannose (Figure 4D and E, respectively).

1-4-6. Effect of acceptor structure on the second mannose addition

To examine the substrate specificity of the second mannose addition, high mannose type oligosaccharides other than the M9A were used as acceptors. The secondary reaction toward each substrate was performed for 6 h under the same conditions as in Figure 3A and the reaction mixtures were separated using an NH2P-50 column (Figure 5). The second mannose was incorporated into the M8B, M8C, M7D

and M6C substrates. In contrast, the acceptors lacking α1,2-mannose at the middle arm, such as M8A, M7A, M7B, M6B and M5A, did not show any second mannose additions. It is likely that the efficiency of this novel reaction depends on the presence of an α1,2-linked mannose residue at the middle arm. These results strongly suggested that the second mannose of the novel product from $Man_9GlcNAc_2$-PA acceptor (peak 3 in Figure 3A) was incorporated with an α1,6-linkage at the α1,3-linked mannose that was located at the middle arm of $Man_{10}GlcNAc_2$-PA, which was produced as a primary product by Och1p, as shown in Figure 4E. Furthermore, the efficiency of the second mannose addition toward M9A and M8B was lower than that toward M8C, M7D and M6C, regardless of the presence of the α1,2-linked mannose at the middle arm (Figure 3A and 5). It is noteworthy that both M9A and M8B have α1,2-linked mannose at the upper arm, in contrast to the structures of M8C, M7D and M6C. Thus, it is likely that the above difference of efficiency may be caused by the steric hindrance of α1,2-linked mannose at the No. 7 position (Figure 2).

Although the M6C substrate was not used as an acceptor under the normal reaction conditions, the second mannose addition occurred more efficiently for M6C than for M9A and M8B. I further analyzed the enzymatic reaction profile of M6C. During the time-course study (Figure 6A), peak A (product A) and peak A' (product A') indicating the first mannose addition were detected as intermediates. To examine the intermediate structures, the fraction containing products A and A' was collected and treated with α1,6-mannosidase, resulting in the conversion of only product A, but not product A', into the M6C substrate (Figure 6B). This result raises the possibility that there are two isomeric forms of product A, i.e., mannosylated at the No. 3 or at the No. 4 position of M6C (see Figure 2). Taking into consideration the original activity of

Och1p, I predict that product A is $Man_7GlcNAc_2$-PA in which the first mannose was incorporated at the No. 3 position of M6C substrate (Figure 6C). I also predict that in product A', the first mannose was added at the No. 5 position, because of the results of α1,6-mannosidase resistance and the second mannose incorporation specificities (Figure 5). Consequently, the synthesis of product B was started by the addition of a mannose residue at the No. 3 position, which was followed by the addition of a second mannose at the No. 5 position (Figure 6C). These results indicate that Och1p preferentially transferred a mannose residue at the lower arm at a high concentration of Och1p, in spite of the lack of α1,2-linked mannose at the lower arm.

1-5. Discussion

Many kinds of mannosyltransferases responsible for the elaboration of outer chain, including Och1p, were identified and characterized by using each protein deficient mutant strain. However, only a few case of recombinant protein have been reported. In this study, I expressed a soluble form of recombinant Och1p that was produced as a secretory protein in the methylotrophic yeast *P. pastoris* and purified. The recombinant protein was enzymatically active and the tendency of the substrate specificities for the first mannose addition was identical to those previously reported (Yoko-o *et al.* 2001). These results supported that Och1p could act without forming heterocomplex, although other mannosyltransferases involved in the synthesis of outer chain elongation formed complexes (Dean 1999).

It is likely that Och1p strictly recognizes its substrates, considering the *in vivo* role of Och1p as an α1,6-mannosyltransferase acting on the ER core type oligosaccharides. In contrast, HPLC analysis of the products of the enzymatic reaction at a high concentration of Och1p revealed that the products contained two molecules of mannose incorporated into $Man_9GlcNAc_2$-PA acceptor. In case of human α1,3-fucosyltransferases (α1,3-FUTs), which transfer a fucose residue to *N*-acetylglucosamine of type 2 chain (Gal-β1,4-GlcNAc) with an α1,3-linkage, were characterized by using 2AB-labeled polylactosamine chain (Gal-β1,4-GlcNAc-β1,3-Gal-β1,4-GlcNAc-β1,3-Gal-β1,4-GlcNAc-2AB; 3LN-AB) as an acceptor (Nishihara *et al.* 1999). The analyses of the substrate specificity showed that FUT9 preferentially fucosylated the distal GlcNAc residue of 3LN-AB, although other

α1,3-FUT members (FUT3, FUT4, FUT5 and FUT6) preferentially fucosylated the inner GlcNAc residue. These results implied that glycosyltransferases have a high degree of specificity for the linkage they form, but each enzyme shows flexibility in its recognition of acceptor substrate. For this reason, it seems reasonable that further mannosylation by Och1p occurs at a different position in addition to the original position. However, this addition was observed under the limited condition that an α1,2-linked mannose at the middle arm is present and an α1,2-linked mannose at the upper arm is absent (Figure 2 and 5). It seems likely that Man-α1,2-Man-α1,3-Man, which is the common partial structure in acceptor oligosaccharides around the mannose transferred, was recognized by Och1p. The structural analyses of M6C products formed at a high concentration of Och1p revealed that the first mannose was mostly incorporated at the lower arm (Figure 6A and C). To further examine this point, chemically synthesized Man-α1,2-Man-α1,3-Man tri-saccharide and its derivative, in which the reducing terminus was either free and modified with β-linked fluorine to mimic the lower arm of native acceptors, respectively, were tried as a competitive inhibitor, but did not inhibit the first and second mannose transfer reactions (data not shown). In contrast, the substrate specificities for the first mannose addition revealed that the upper rather than the lower arm is important for the transfer of a mannose residue by Och1p, although the mannose was incorporated into the lower arm. Therefore, it is possible that Och1p does not recognize the partial structure, such as Man-α1,2-Man-α1,3-Man, but the entire structure of high mannose type oligosaccharide.

The gene encoding α1,6-mannosyltransferase was reported not only in *S. cerevisiae* but also in *S. pombe* and *Y. lipolytica* (Yoko-o *et al.* 2001; Barnay-Verdier *et*

al. 2004). In addition, the homologous to Och1p are found in many kinds of yeast by BLAST search in the DNA Data Bank of Japan. At present, however, the α1,6-mannosyltransferase activity has been characterized only for *S. cerevisiae* Och1p (ScOch1p) and *S. pombe* Och1p (SpOch1p) by *in vitro* assays. The substrate specificity of ScOch1p is significantly different from that of SpOch1p (Yoko-o *et al.* 2001), although both Och1 proteins act as an α1,6-mannosyltransferase that is essential for the outer chain elaboration. To test the incorporation of a second mannose by SpOch1p, I prepared a recombinant SpOch1p, which was similarly expressed in *P. pastoris* as a secreted protein. The recombinant SpOch1p had a catalytic activity of the first mannose addition to $Man_9GlcNAc_2$-PA, although the specific activity was about 20 times lower than that of ScOch1p. However, it could not transfer a second mannose in the presence of 150 μg/ml enzyme (data not shown). This result further supported that the contaminants did not transfer a second mannose, since I purified SpOch1p by the procedures similar to ScOch1p. It is known that in *S. pombe* $Man_9GlcNAc_2$ is not trimmed by the ER α-mannosidase after the removal of three glucose residues (Ballou *et al.* 1994; Ziegler *et al.* 1994; Movsichoff *et al.* 2005), indicating that $Man_9GlcNAc_2$ is an original acceptor substrate for SpOch1p. In contrast, *S. cerevisiae* has an ER α-mannosidase that hydrolyses the α1,2-linked mannose at the middle arm, leading to the formation of $Man_8GlcNAc_2$ (Herscovics 1999). The role of α-mannosidase was studied by examining the effect of disruption of the *MNS1* gene encoding ER α-mannosidase on glycosylation, and the results suggested that the mannose removal is not essential for the maturation of *N*-linked oligosaccharide (Puccia *et al.* 1993). However, it seems to be important for ER α-mannosidase to remove the α1,2-linked mannose of $Man_9GlcNAc_2$ to generate $Man_8GlcNAc_2$, because the first mannose

addition was more efficient toward the M8A acceptor than the M9A acceptor, and the second mannose addition was not observed with M8A.

Multiple amino acid sequence alignment revealed that SpOch1p lacks three regions that are present in ScOch1p (Yoko-o *et al.* 2001). It is likely that these regions are involved in both the substrate specificities and the second mannose incorporation activity. It will be interesting to address whether the insertion of the above three regions into SpOch1p would change the enzymatic properties of SpOch1p into those of ScOch1p.

It is noteworthy that the incorporation of first and second mannose by Och1p was observed only into the high mannose type oligosaccharide, but not into the oligomannose acceptors that are recognized by other mannosyltransferases like Kre2p/Mnt1p. These results support further understanding of the molecular mechanism of the substrate recognition and enzymatic reaction, although the biological function of the second mannose addition of ScOch1p is still unknown. Crystal structure analysis of recombinant Och1p is necessary to answer these questions.

CHAPTER 2

Use of novel selenomethionine-resistant yeast to produce selenomethionyl protein suitable for structural analysis

2-1. Summary

Yeast is widely used as a host cell to determine the tertiary structure of recombinant eukaryotic proteins, because of its ability to undergo post-translational modifications such as glycosylation. However, attempts to use yeast expression system for preparation of selenomethionine-incorporated derivatives, which can help solve phase problems in protein crystallography, have been limited due to the toxic effect of selenomethionine. Here, a selenomethionine-resistant *Pichia pastoris* mutant that was also resistant to selenate was isolated. Human lysozyme that was expressed by the mutant under the control of constitutive promoter contained selenomethionine at 65% occupancy, and this amount was sufficient for use as a selenomethionine derivative for single-wavelength anomalous dispersion phasing.

2-2. Introduction

Proteins whose methionine residues are replaced with selenomethionine (SeMet) are useful for solving phase problems for X-ray crystallography by a single-wavelength anomalous dispersion (SAD) or multi-wavelength anomalous dispersion (MAD) method (Hendrickson *et al.* 1990; Rice *et al.* 2000). Expression of SeMet derivatives has been achieved routinely in *E. coli*, however, eukaryotic proteins that receive post-translational modifications, such as glycosylation, often failed to be expressed as functional proteins. To overcome this fundamental limitation, yeasts are used to express eukaryotic proteins because yeasts have subcellular organelles common to eukaryotes. Additional benefits of a yeast expression system include simple culture conditions and straightforward scale-up to fermentation. These advantages contribute to protein structure analysis because crystallization requires a large amount of highly purified protein.

Recent studies have demonstrated that the deletion of genes involved in sulfur amino acid synthesis results in enhanced tolerance of SeMet, however, this approach requires external addition of *S*-adenosylmethionine (AdoMet) or cysteine that is expensive and unstable compound (Malkowski *et al.* 2007; Bockhorn *et al.* 2008). The SeMet-resistant mutants able to grow in the absence of AdoMet and cysteine were isolated as spontaneous mutants (Cherest *et al.* 1973). However, such mutants showed a 10-fold increase of intracellular methionine pools, which resulted from overexpression of enzymes involved in sulfate assimilation (Figure 7). This finding suggests that SeMet incorporation by the mutants might be inhibited by newly synthesized methionine. Therefore, it is important to isolate SeMet-resistant mutants without enhanced sulfate

assimilation.

Methylotrophic yeast *P. pastoris* possesses advantages over *S. cerevisiae* for the production of recombinant proteins. One reason for this is that *P. pastoris* has the ability to reach much greater cell densities than *S. cerevisiae*, which may improve overall yields. Selenomethionyl dextranase from *Penicillium minioluteum* or β-mannanase from *Mytilus edulis* was produced by the non-mutageneized *P. pastoris*, with 40–50% of SeMet incorporation. However the productivity of its SeMet derivatives was considerably lower than that of SeMet-unlabeled proteins (Larsson *et al.* 2002; Xu *et al.* 2002).

This study describes the isolation of mutants in *P. pastoris* that were suitable for SeMet incorporation into the recombinant protein, which was expressed under the control of constitutive promoter. To obtain the desired mutants, SeMet-resistant mutants were initially isolated by spontaneous mutation. Then the SeMet-resistant mutants without an enhanced sulfate assimilation pathway were obtained by further screening in the presence of selenate. The mutant obtained showed double-resistance to both SeMet and selenate. To assess the mutant availability, human lysozyme (HLY), which is unsuitable for expression in *E. coli* due to its peptidoglycan hydrolytic activity, was produced as a secreted protein by the mutant. SeMet incorporation into HLY was confirmed by mass spectrometry and amino acid composition analysis. In addition, the measured Bijvoet differences were sufficient to determine two selenium sites and to obtain initial phases for automatic model building.

2-3. Materials and Methods

2-3-1. Culture media and strains

Pichia pastoris SMD1168 strain was used as a parental strain. Yeast cells were cultured in BMGY or YPD supplemented with sodium selenate (Wako, Osaka, Japan) or L-selenomethionine (Nacalai Tesque, Kyoto, Japan). For mutant screening, SD medium was used. To produce a selenomethionyl protein, another synthetic complete medium (Larsson *et al.* 2002) supplemented with 0.1 M potassium phosphate buffer (pH 6.0) was used.

2-3-2. Construction of expression vectors and strains

To integrate the expression vector into the *his4* locus and constitutively express recombinant proteins, the vectors were constructed as follows. The pPIC9 plasmid (Invitrogen) was digested with *Eco*RV and *Nae*I, and then the DNA fragment containing *HIS4* was ligated into the corresponding sites of pBluescript II SK(+) (Stratagene), yielding plasmid pBS-HIS4. The pGAPZαC plasmid (Invitrogen) was digested with *Bgl*II and *Bam*HI, and then the DNA fragment containing the promoter region of the gene (*P. pastoris GAP*) encoding glyceraldehyde-3-phosphate dehydrogenase was ligated into the *Bam*HI-digested pBS-HIS4. The resulting plasmid, pGHA1, was digested with *Pci*I and *Spe*I, and self-ligated after blunting, yielding plasmid pGHA3. The HLY gene containing the region from amino acids 19 to 148 was synthesized with its codon optimized for yeast expression (unpublished data). To express HLY under the control of the *AOX1* and *GAP* promoters, the DNA fragment was cloned into the *Xho*I and *Not*I sites of pPIC9 and pGHA3, yielding plasmids

pPIC9-HLY and pGHA3-HLY, respectively. Using this construct, recombinant HLY was expressed with an N-terminal secretion signal (α-factor prepro peptide) for secretion into the medium. After the expression vectors were linearized with the *Stu*I, transformation of *P. pastoris* was conducted by LiCl method.

2-3-3. Immunoblots

Samples were denatured with an equal volume of 2× loading buffer for 5 min at 99°C, and then separated by SDS-PAGE. After the proteins were transferred to a PVDF membrane, HLY was detected with anti-human lysozyme polyclonal antibody (1:5000; DAKO A/S, Glostrup, Denmark) and alkaline phosphatase-conjugated goat anti-rabbit IgG (1:10000; Rockland Immunochemicals, Gilbertsville, PA, USA). Immunoreactive bands were visualized by chemiluminescence with CDP-Star reagents.

2-3-4. Isolation of SeMet-resistant strains

P. pastoris was cultivated overnight in YPD liquid media. The cells were washed and resuspended in sterilized water. One hundred microliters of cell suspension (approximately 4×10^6 cells) were plated on SD medium lacking methionine (SD-Met) containing 3.13 μg/ml of SeMet, followed by incubation at 30°C. After six days, all growing cells were resuspended in sterilized water and plated again (approximately 5×10^6 cells) on SD-Met media containing 12.5 μg/ml of SeMet. After incubation at 30°C for four days, 160 colonies were isolated and used as SeMet-resistant strains.

2-3-5. Selenomethionyl HLY expression and purification

The HLY expression strain was grown in 5 ml YPD at 30°C for 16 h. The

cells were then washed with sterilized water and 5×10^5 cells were inoculated into 200 ml of synthetic complete media containing 50 μg/ml of SeMet or methionine. After five days of cultivation at 30°C, the culture supernatants were loaded into a dialysis tube (MWCO 3500) and dehydrated in the presence of PEG6000. The concentrated sample was dialyzed against 20 mM sodium phosphate (pH 6.0), and then loaded on HiTrapSP (5 ml; GE Healthcare) equilibrated with the same buffer. HLY was eluted using a linear gradient from 0 to 500 mM of sodium chloride. The fractions containing HLY were collected and desalted by milliQ water using a HiTrap desalting column (5 ml; GE Healthcare). The purified protein was freeze-dried and stored at 4°C until use.

2-3-6. Analysis of SeMet content

SeMet incorporation into the protein was estimated using a decrease in the relative methionine content. Amino acid analyses were performed on a Hitachi L-8500 amino acid analyzer (Hitachi High-Technologies, Tokyo, Japan), after hydrolysis *in vacuo* with 6 N HCl at 110°C for 22 h.

2-3-7. Mass spectrometry

A sample of 12.5 μg of freeze-dried HLY was dissolved in 5 μl trypsin solution (20 μg/ml trypsin in 20 mM ammonium hydrogen carbonate) and incubated at 37°C overnight. A portion of the trypsin-treated sample was mixed with α-cyano-4-hydroxycinnamic acid in 50/50 acetonitrile/water (v/v) containing 0.5% TFA, followed by analysis using an Ettan MALDI-ToF Pro instrument (GE Healthcare). Average mass was used to confirm the tryptic peptides of HLY.

2-3-8. Crystallization, data collection and structure determination

Crystallization was performed according to the procedure described by Inaka *et al*. (1991) with the following modifications. HLY crystals were grown using a hanging-drop vapor-diffusion method at 20°C. A 1-μl droplet of protein at 25 mg/ml was mixed with an equal volume of the reservoir solution containing 30 mM sodium phosphate (pH 6.0) and 1.8 M NaCl. Crystals were soaked in a reservoir solution containing 15% (v/v) glycerol as a cryo-protectant. A data set was collected with a synchrotron radiation beamline instrument (PF-BL-17 in KEK, Japan). The data were processed up to 1.25 Å resolution with the HKL2000 program (Otwinowski and Minor 1997).

The structure of HLY was solved using the SAD phasing method. Two selenium sites were identified by the SHELXD program (Sheldrick 2008), and used for phase calculation in the Mlphare program in the CCP4 suite (CCP4 1994). After phase improvement through density modification by the DM program (Cowtan 1994), the initial model containing 124 residues was automatically generated by the ARP/wARP program (Perrakis *et al.* 1999). Remaining residues were built manually using the COOT program (Emsley and Cowtan 2004). The final model was obtained by seven cycles of model building using COOT followed by refinement with the REFMAC program (Murshudov *et al.* 1997).

2-4. Results

2-4-1. Isolation of SeMet-resistant mutants suitable for selenomethionyl protein expression

Attempts to reproduce selenomethionyl protein using the wild-type *Pichia pastoris* revealed that the expression level was improved under the control of the *GAP* promoter that expresses constitutively, rather than that under the control of the methanol-inducible *AOX1* promoter (Figure 8). When a secreted protein is expressed under the control of a constitutive promoter, replacement of the initial growth medium with SeMet-labeling medium is important to remove SeMet-unlabeled proteins. The advantages of the *P. pastoris* expression system, such as the ease of large-scale cultivation, indicate that the isolation of SeMet-resistant mutants in *P. pastoris* is practical.

Pichia pastoris SMD1168 strain did not readily proliferate in the presence of 3.13 μg/ml SeMet on SD-Met, and did not grow at all in the presence of 12.5 μg/ml SeMet (data not shown). By subculturing SMD1168 cells on medium containing a greater concentration of SeMet (see Materials and Methods), mutants that grew on SD-Met medium containing 12.5 μg/ml SeMet were isolated. The mutants (denoted as SMR: SeMet-resistant mutant) grew on YPD without AdoMet and YPD medium containing 50 μg/ml SeMet (Figure 9).

Because SeMet-resistant mutants with an enhanced ability to assimilate sulfate were isolated by a spontaneous mutation in *S. cerevisiae* (Cherest *et al.* 1973), it is likely that SMR mutants also increase the methionine pools. Such mutants, unlike wild-type cells, possess a sensitivity toward selenate, which is used as a toxic sulfate

analogue, in rich medium (Kuras *et al.* 2002). A selenate resistance assay revealed that most of the SMR mutants were sensitive to selenate, whereas SMR-46, SMR-94 and SMR-98 possessed resistance to selenate (Figure 9). Because SMR-94 was most resistant to selenate, the sulfate assimilation ability of SMR-94 was minimally enhanced. Therefore, the SMR-94 strain was used for selenomethionyl protein production in the following experiment.

2-4-2. Evaluation of SeMet-resistant strain

HLY was expressed by the SMR-94 strain as a secreted protein. The growth rate of SMR-94 cells was significantly slower in the presence of SeMet than in the presence of methionine; however, SMR-94 cells could produce recombinant HLY in the culture medium. After five days of cultivation, approximately 400 μg of purified HLY was consistently obtained from 200 ml of culture broth. The productivity of SeMet derivative of HLY was equal or slightly less than the SeMet-unlabeled HLY produced by parental SMD1168 cells. Qualitative analysis of selenium incorporation into HLY was conducted using MALDI-TOF mass spectrometry (Figure 10). The peak at *m/z* 1825 was assigned to a protonated molecular ion of the disulfide-bonded peptide (molecular weight 1824) containing 29-Met. This peak was increased by 47 (*m/z* 1872) in HLY produced by SMR-94 cells, corresponding to replacement of sulfur by selenium, indicating partial incorporation of SeMet into the HLY protein.

To estimate the extent of SeMet incorporation, the amino acid composition of HLY was determined. The SeMet content was deduced on the basis of residual methionine because SeMet does not contribute to methionine content (Larsson *et al.* 2002; Xu *et al.* 2002). As shown in Table 4, amino acid composition (without

methionine) of HLY produced by SMR-94 cells was nearly equal to that of HLY produced by SMD1168 cells. In contrast, the methionine composition of HLY produced by SMR-94 decreased to 0.6 mol%. Based on these results, the incorporation rate of SeMet was estimated to be 65%.

2-4-3. Determination of selenomethionyl HLY structure

To evaluate the usefulness of the SMR-94 strain for X-ray crystallography, determination of the HLY protein structure was attempted using the SAD phasing method. The X-ray absorption spectrum of the crystal showed the selenium *K* edge at 0.97929 Å; X-ray diffraction data then were collected at that wavelength. The two selenium sites were clearly identified by the SHELXD program and used for phase calculation. The electron density map obtained after phase refinement was clear enough for model building (Figure 11A). Indeed, the ARP/wARP program was able to trace 95% of the HLY polypeptide chain. To confirm the sites of selenium atoms in HLY molecules expressed by SMR-94 cells, an anomalous difference Fourier map was created (Figure 11B). The electron densities contoured at 10σ were observed at the sulfur atoms of both methionine residues, indicating that replacement of methionine with SeMet using SMR-94 cells was sufficient for SAD phase determination.

2-5. Discussion

In this study, the usefulness of SeMet-resistant mutants isolated from *P. pastoris* for selenomethionyl protein production was demonstrated. Since SMR-94 cells did not exhibit the methionine auxotrophic phenotype (data not shown), it is likely that SeMet incorporation by SMR-94 was incomplete. However, the crystal structure of HLY produced by SMR-94 was successfully solved using the SAD phasing method. Amino acid analysis revealed that SeMet incorporation into HLY by SMR-94 (65%) was improved compared to that into dextranase (50%) or into β-mannanase (40%) by wild-type *P. pastoris* (Larsson *et al.* 2002; Xu *et al.* 2002), although the residual methionine composition based on amino acid analysis might be insufficient to estimate SeMet content accurately. Since the incorporation levels of these proteins were estimated based on the same procedures, SMR-94 appears superior to wild-type *P. pastoris* for producing SeMet derivatives. In addition, SMR-94 proliferates in the absence of AdoMet or cysteine, unlike other SeMet-resistant mutants in *S. cerevisiae* (*sam1*Δ *sam2*Δ and *cys3*Δ mutants). These advantages will expand the applicability of selenomethionine labeling to eukaryotic proteins through a simple and inexpensive process, and thus contribute to the field of structural biology.

To produce recombinant proteins with a high level of SeMet incorporation, media lacking methionine should be used. However, the recombinant HLY was barely expressed under the control of the *AOX1* promoter with synthetic complete medium containing methionine in parental SMD1168 cells, although the culture conditions were similar to those for the production of dextranase (Larsson *et al.* 2002). In *P. pastoris*, the *AOX1* and *AOX2* genes code for alcohol oxidase, and the *AOX1* gene product

accounts for the majority of alcohol oxidase activity in the cells (Cregg *et al.* 1989). Consequently, the strain with a mutation at *AOX1* shows a slow-growth phenotype on methanol medium. For dextranase production, the expression vector was inserted into the *AOX1* locus to remove the *AOX1* coding region, which resulted in a significant reduction of alcohol oxidase activity in cells. In contrast, the HLY expression vector was inserted into the *his4* locus of the chromosome to retain the wild-type *AOX1* gene. Host cells possessing alcohol oxidase are assumed to express recombinant proteins efficiently in the presence of methanol, in contrast to cells lacking alcohol oxidase. However, the recombinant HLY was scarcely produced by the host cells that can utilize methanol as a carbon source (Figure 8). A report indicates that *aox1* mutant cells are superior to wild-type cells for D-alanyl-D-alanine carboxypeptidase production (Despreaux and Manning 1993). The reason for the greater productivity in *aox1* mutant cells compared to that in wild-type cells is difficult to explain.

When selenomethionyl proteins are expressed by the wild-type cells, the productivity of recombinant proteins is significantly decreased due to the cell growth inhibition caused by SeMet toxicity. To compensate the decreased productivity, the wild-type cells need to be pre-cultured in SeMet-free medium until a late logarithmic or stationary phase prior to the cultivation in SeMet-containing medium. When desired proteins are overexpressed under the constitutive promoter, the process to remove proteins that are expressed during the pre-culture period is important to prevent contamination of SeMet-unlabeled proteins. However, I demonstrated that HLY constitutively expressed by SMR-94 cells contained 65% of SeMet, even though the culture medium was not exchanged during expression of SeMet-labeled HLY. This result suggests that SMR-94 has a potential to produce SeMet derivatives of not only

secretory protein, HLY, but also of general proteins because $tRNA^{Met}$ is assumed to be charged with SeMet as well as methionine by methionyl tRNA synthetase, Accordingly, the high ability of SMR-94 to incorporate SeMet into proteins may be helpful not only to produce secretory proteins but also intracellular proteins, the latter of which cannot be removed by the medium exchange. In addition, the effective production yield of SeMet derivatives in this system is an important advantage over the previously reported wild-type *P. pastoris* system (Larsson *et al.* 2002; Xu *et al.* 2002).

The reasons for the SeMet resistance of SMR-94 cells and their ability to produce HLY containing SeMet are unclear. However, the strain is useful for determining the tertiary structure of proteins, especially mammalian proteins difficult to express in *E. coli*. The analysis of the mutation sites in SMR-94 strain is important to produce selenomethionyl proteins stably and efficiently; however, it is difficult because little genome information and few tools are available for *P. pastoris*. Since *S. cerevisiae* mutants that exhibit phenotypes similar to the *P. pastoris* SMR-94 mutant were obtained, I further characterized the SeMet resistance mechanism in the following chapter.

CHAPTER 3

Characterization of novel selenomethionine-resistant mutant in *Saccharomyces cerevisiae* suitable for selenomethionyl protein production

3-1. Summary

Selenomethionine (SeMet) is toxic amino acid, but proteins containing SeMet are valuable for phase determination by a single- or multi-wavelength anomalous dispersion method. Yeast has a potential to overcome the above discrepancy by using SeMet-resistant mutants. Previously, I isolated *Pichia pastoris* SMR-94 that were resistant to both SeMet and selenate as a novel mutant. The mutant was able to grow without sulfur amino acids and to produce the SeMet-labeled protein suitable for X-ray crystallography. To understand SeMet-resistant mechanism of *Pichia pastoris* SMR-94, I further isolated two types of SeMet-resistant mutants in budding yeast *Saccharomyces cerevisiae*, one is resistant to both SeMet and selenate (SRY5-7) and the other is resistant to SeMet but sensitive to selenate (SRY5-3). By a genetic analysis, a mutant allele of *MUP1* encoding high affinity methionine permease and *SAM1* encoding *S*-adenosylmethionine synthetase were identified in SRY5-7 (*mup1-100*) and SRY5-3 (*sam1-224*), respectively. Microarray analysis revealed that genes involved in sulfur amino acid metabolism, especially sulfate assimilation, were significantly up-regulated in both *mup1-100* and *sam1-224* as compared with wild-type, but the expression level in *mup1-100* was lower than that in *sam1-224*. On the other hand, *mup1-100* cells have the ability enough to incorporate external methionine, even though the cells lacked the function of high affinity methionine permease. These results suggest that *mup1* mutant is a suitable host to produce proteins with a high content of SeMet for X-ray crystallography without any supplementation of sulfur amino acids.

3-2. Introduction

SeMet-labeled proteins are valuable for SAD or MAD phasing in X-ray crystallography; however, SeMet is known to be toxic for living cells, especially eukaryotic cells, while the toxic mechanism is not yet clear. The use of SeMet-resistant mutants is assumed to overcome this fundamental limitation and to be an attractive host for the production of SeMet-labeled proteins. In case of yeast, it is thought that there are two mechanisms to overcome SeMet toxicity. One is that *sam1* mutation leads cells to overproduce endogenous methionine, resulting in alleviating SeMet toxicity (Cherest *et al.* 1973). The other mechanism is that blocking the synthesis of metabolites containing selenium, such as *Se*-adenosylselenomethionine, allows yeast cells to grow in the presence of SeMet because *sam1*Δ *sam2*Δ lacking the ability to convert SeMet to *Se*-adenosylselenomethionine (see Figure 7) showed a resistance to SeMet (Malkowski *et al.* 2007). Most recent work demonstrated that the deletion of *CYS3*, which blocks the conversion of cystathionine to cysteine (see Figure 7), also gave a SeMet-resistant phenotype (Bockhorn *et al.* 2008). To produce selenomethionyl proteins suitable for X-ray crystallography, the mutants that is able not only to overcome SeMet toxicity but also to incorporate SeMet into target proteins with a high SeMet content are required as an expression host. Blocking the sulfur amino acid metabolic pathway will contribute to the effective incorporation of SeMet into proteins, however, a supply of sulfur amino acids is essential for such mutants both to produce SeMet-labeled proteins and to maintain cell growth. In addition, *sam1* mutant that is able to grow in the absence of sulfur amino acids is unfavorable for the production of SeMet-labeled protein because SeMet incorporation into protein is inhibited by overproduced methionine. Accordingly,

the repressive control of the sulfur amino acid metabolism is important to produce proteins with a high content of SeMet.

I previously isolated novel SeMet-resistant mutant in *P. pastoris* for preparation of proteins containing SeMet, which is sufficient for phase determination in X-ray crystallography. The mutant (*P. pastoris* SMR-94) was resistant to both SeMet and selenate, suggesting that the mutant overcame SeMet toxicity without enhanced methionine synthesis, different from *S. cerevisiae sam1* mutant that is sensitive to selenate. SMR-94 has advantages for a simple and cost-effective method to produce SeMet-labeled proteins, because the mutant is autotrophic to sulfur amino acids, unlike *sam1*Δ *sam2*Δ and *cys3*Δ mutants.

Here I describe the functional characterization of *S. cerevisiae* SRY5-7 that showed a similar phenotype to *P. pastoris* SMR-94 cells and the genetic approach to identify the mutated gene. The results demonstrate that the cellular ability of methionine synthesis is up-regulated by the recessive mutation of *MUP1* to the extent where the cells were able to grow in the presence of 10 mM selenate and that SRY5-7 cells have an ability to incorporate a sufficient amount of external methionine. Combined results support that the *mup1* mutant that shows double resistance to SeMet and selenate is a novel host cells to produce SeMet-labeled proteins for X-ray crystallography.

3-3. Materials and Methods

3-3-1. Culture media and strains

Yeast cells were cultured in YPAD or SD medium. The sodium selenate (Wako) was added to YPAD at a final concentration of 10 mM. The L-selenomethionine (Nacalai Tesque) was added to SD-Met at a final concentration of 5–100 μg/ml. LA-agar plate contained 0.3% Bacto-peptone, 0.5% Bacto-Yeast Extract, 4% glucose, 0.02% ammonium sulfate, 0.1% lead acetate, 0.01% adenine sulfate and 2% agar.

3-2-2. Isolation of SeMet-resistant mutants in *S. cerevisiae*

S. cerevisiae W303-1A was cultivated overnight in YPAD liquid media. The cells were washed and resuspended in sterilized water. One hundred microliters of cell suspension (approximately 2×10^6 cells) were plated on SD-Met media containing 5 μg/ml of SeMet, followed by incubation at 30°C. After four days, all growing cells were replicated on SD-Met media containing 100 μg/ml of SeMet. After incubation at 30°C for four days, SRY5-3 and SRY5-7 were isolated and used as SeMet-resistant strains.

3-3-3. Genetic analysis

To obtain diploid strains, *S. cerevisiae* haploid SeMet-resistant mutants derived from W303-1A (*MAT***a**) were mixed with W303-1B cells (*MAT*α) and cultured on YPAD plate for one day at room temperature. Diploid cells grown on YPAD plate were picked up with sterilized toothpick and transferred onto a SPO plate (1% [w/v] potassium acetate and 2% [w/v] agar) and incubated for three days at 25˚C. The

sporulrated cells were suspended in sterilized water. Small amounts of Zymolyase 100T were added into the suspension and incubated for 1 min at room temperature to digest cell wall of ascus. The suspension was spotted on YPAD plates, and dried up under a laminar flow cabinet. Tetrad ascospore was dissected individually with micromanipulator under a microscope. The individual ascospore haploid cell was cultured independently and assayed their phenotype.

3-3-4. Plasmid construction for *S. cerevisiae*

A DNA fragment, which contains *SAM1* open reading frame (ORF), a 1.0-kbp upstream region and 0.6-kbp downstream regions, was amplified by PCR using two primers, SAM1-FW (5'-AAAACCCGGGGCACAGGAAGAACACGTATC-3') and SAM1-RV (5'-TTTTCCCGGGCGATAGCGTAAACGAAGAAG-3'). The PCR product was digested with *Sma*I and purified from the corresponding band (2.7-kbp) on the agarose gel. The purified DNA fragment was cloned into the corresponding site of pRS316, and its DNA sequence was confirmed using an ABI PRISM 3100 Genetic Analyzer (Applied Biosystems, Foster, CA, USA).

A DNA fragment, which contains *MUP1* ORF, a 0.9-kbp upstream region and 0.6-kbp downstream regions, was amplified by PCR using two primers, MUP1-FW (5'-AAAACCCGGGGTCGGCGACAAACTAGAAG-3') and MUP1-RV (5'-TTTTCCCGGGGGAAGACAGCATCGTATTGT-3'). The PCR product was digested with *Sma*I and purified from the corresponding band (3.2-kbp) on the agarose gel. The purified DNA fragment was cloned into the corresponding site of pRS316, and its DNA sequence was confirmed as described above.

3-3-5. Microarray analysis

Yeast cells were cultivated in YPAD medium and harvested at mid-logarithmic phase (A_{600} = 0.7–1.0). Total RNA was isolated with the RNAeasy kit (QIAGEN) according the manufacture's protocol. RNA labeling was conducted by using Amino Allyl MessageAmp™II aRNA Amplification Kit (Applied Biosystems). Briefly, cDNA was synthesized with Oligo(dT) primer containing T7 promoter sequence. After the single-strand cDNA was converted into double-stranded transcription templates, amino-allyl RNA was synthesized with incorporation of amino-allyl UTP by T7 RNA polymerase. The amino-allyl RNA was coupled to *N*-hydroxysuccinimide conjugated with Cy3 (for wild-type) or Cy5 (for SRY5-3 and SRY5-7) to generate fluorescent-labeled RNA. The 3D-Gene Yeast Oligo chip (Toray, Tokyo, Japan) was used for hybridization. The slides were scanned using a GenePix 4000B and analyzed using GenePix Pro (Molecular Devices, Sunnyvale, CA). Data for each spot were corrected for background and the data from Cys3 and Cy5 were normalized to the total intensity. These data were acquired at the New Frontiers Research Laboratories (Toray). The genes that were up-regulated or down-regulated more than 3-fold were judged as differentially expressed genes.

3-3-6. Identification of the genes that are responsible for SeMet resistance

To identify the genes involved in SeMet resistance in SRY5-3, SRY5-3 cells were transformed with a centromeric yeast genomic DNA library (*URA3* marker) and plated on SDCA medium lacking uracil containing 10 mM selenate. Four plasmids were recovered from the independent colonies that could grow in the presence of selenate. The DNA sequence analysis revealed that all plasmids independently contained *SAM1*

or *SAM2* ORF. Further sequencing analysis of the PCR fragments of *SAM1* and *SAM2* amplified from SRY5-3 genomic DNA identified a single base substitution at the *SAM1* ORF (*sam1-224*).

To identify the mutation sites of SRY5-7 cells, the TKY358 cells in which *MET17* gene was further disrupted in SRY5-7 cells were transformed with a centromeric yeast genomic DNA library and plated on SD medium lacking uracil (SD-Ura) containing 5 μg/ml of methionine and 10 mM selenate. Since SRY5-7 cells in which *MET17* gene was not disrupted were able to grow under the culture condition (Figure 14B), the transformants harboring the plasmid containing *MET17* ORF, but not containing the gene involved in SeMet resistance, were expected to be isolated. In order to exclude the unfavorable transformants, all transformants were replicated onto SD-Ura and LA-agar plates. The plasmids were recovered from the cells that showed dark-brown colonies on LA-agar plate because it is reported that H_2S, which is accumulated in cells lacking Met17p, causes formation of PbS (Ono *et al.* 1991). The DNA sequence analysis revealed that the transformants harbored the plasmids containing *MUP1*, *RSC1* and *LST7* ORFs. Further sequence analysis of the PCR fragment of *MUP1* amplified from SRY5-7 genomic DNA identified a single base substitution at the *MUP1* locus (*mup1-100*).

3-3-7. Measurement of methionine uptake

The methionine uptake was measured as described by Isnard *et al.* (1996) with some modifications as follows. Briefly, the overnight cultured cells were inoculated to the minimal medium (2% [w/v] glucose, 0.67% [w/v] Bacto-Yeast Nitrogen Base w/o amino acids) supplemented with amino acids and nucleic acid bases

required for the complementation of the auxotrophy of each strain, and cultured until 0.9–1.1 A_{600}. The assay was started by mixing 495 μl of cell culture with 5 μl of methionine solution containing 30.2 kBq of [methyl-^{3}H] methionine (3.03 TBq/mmol; PerkinElmer, Boston, MA, USA) at a final concentration of 20 or 250 μM. Aliquot (95 μl) of the mixtures were withdrawn, then cells were filtered onto a glassfiber filter (GF/C; Whatman, Kent, United Kingdom) and washed twice with 5 ml of ice-cold water. The radioactivity on the glassfiber filter was quantified using a liquid scintillation counter (ALOKA, Tokyo, Japan). The data were normalized for the differences in cell density (1.0 A_{600} = 1 × 10^{7} cells).

3-4. Results

3-4-1. Isolation of SeMet-resistant mutants in *S. cerevisiae*

SeMet-resistant mutants that grew on SD-Met medium containing 50 μg/ml of SeMet were isolated by subculturing W303-1A cells on SD-Met medium containing a greater concentration of SeMet as described in Materials and Methods (Figure 12A). A selenate resistance assay of the isolated mutants revealed that SRY5-3 was sensitive to selenate, whereas SRY5-7 showed resistance to selenate (Figure 12B), suggesting that the ability of sulfate assimilation is hardly enhanced in SRY5-7. The diploid cells SRY5-7d generated from crosses between SRY5-7 and W303-1B changed to SeMet-sensitive phenotype similar to wild-type haploid cells (Figure 12A). In case of SRY5-3, diploid cells SRY5-3d showed not only SeMet-sensitive but also selenate-resistant phenotypes. The dissection of the diploids revealed that both SRY5-3 and SRY5-7 were segregated 2^{+}:2^{-} for SeMet-sensitivity in these crosses (Figure 12C and D). These results indicated that the SRY5-3 and SRY5-7 acquired SeMet resistance due to the single-gene recessive mutation, respectively.

3-4-2. Global change of gene expression in SeMet-resistant mutants

I first performed DNA microarray analysis to characterize the global change at the transcriptional level in mutant cells. Genes that were differently expressed in mutant cells as compared with wild-type cells included 61 up-regulated genes and 223 down-regulated genes in selenate-sensitive mutant (SRY5-3; differentially expressed genes are summarized in Table 5 and up-regulated genes are listed in Table 6). The analysis by using Gene Ontology (GO) Term Finder at *Saccharomyces cerevisiae*

Genome Database (SGD; http://www.yeastgenome.org/) revealed that the up-regulated genes significantly shared some categories for sulfur amino acids metabolism, but down-regulated genes did not share any GO terms. The result is consistent with the selenate-sensitive phenotype of SRY5-3 due to the enhancement of sulfate assimilation. In case of selenate-resistant mutant (SRY5-7), 17 genes were up-regulated and 248 genes were down-regulated more than 3-fold as compared with wild-type cells (differentially expressed genes are summarized in Table 5 and up-regulated genes are listed in Table 7). For the down-regulated genes, no significant GO terms were found, but it was noteworthy that 10 genes were involved in sulfur amino acid metabolism.

I further analyzed the difference of the gene expression between each mutant (Figure 13). The expression level of genes involved in sulfur amino acid metabolism (GOID: 97) of SRY5-7 was lower than that of SRY5-3, although no significant differences were observed in the genes involved in synthesis for aspartate family amino acids (GOID: 9067), serine family amino acids (GOID: 9070), aromatic amino acids (GOID: 9073), histidine (GOID: 9076), branched chain amino acids (GOID: 9082) and for glutamine family amino acid (GOID: 9084). These results indicated that the mutant allele responsible for SeMet resistance of SRY5-7 induced endogenous methionine synthesis at a transcriptional level, even though the extent of activation was lower than that in selenate-sensitive SRY5-3 cells.

3-4-3. Necessity of *de novo* synthesized methionine in SeMet-resistant mutants

The above results raised one plausible explanation for the SeMet resistance of SRY5-7, that the enhancement of methionine synthesis through sulfate assimilation pathway might increase intracellular methionine pool, causing the alleviation of SeMet

toxicity. To address the possibility, *MET6* gene was disrupted in SeMet-resistant mutants to block the conversion of homocysteine to methionine (Figure 7). In yeasts, it is known that homocysteine is synthesized from two different compounds, namely, sulfide or cystathionine (Figure 7). To further identify from which homocysteine was synthesized, *MET17* encoding *O*-acetyl homoserine sulfhydrylase or *STR3* encoding cystathionine β-lyase was disrupted. I found that the deletion of *MET6* or *MET17* caused a loss of SeMet-resistant phenotype of SRY5-7, but not the deletion of *STR3* (Figure 14A). In addition, the similar results were found in SRY5-3 in which endogenous methionine was overproduced. These results indicated that SRY5-7 essentially depended on the newly synthesized methionine from sulfate to alleviate SeMet toxicity, as well as SRY5-3 did.

3-4-4. Identification of genes responsible for SeMet resistance

To identify the gene responsible for SeMet resistance of SRY 5-3, a yeast genomic DNA library on a centromeric plasmid was introduced into SRY5-3 cells. All positive clones in the presence of selenate harbored the plasmids containing *SAM1* or *SAM2* ORF, which is a redundant gene encoding AdoMet synthetase. Sequencing of the PCR fragments amplified from SRY5-3 chromosomal DNA to assess the mutation at *SAM1* or *SAM2* revealed a point mutation of the glycine residue at 267 to cysteine (GGT changed to TGT) of *SAM1* ORF (*sam1-224*, Figure 15A and B).

It is impossible to identify the mutated gene in SRY5-7 cells by the same procedure in which *sam1-224* was identified as a mutant allele of SRY5-3 cells, because SRY5-7 mutant cells showed a selenate resistance, indicating that the negative screening of the SeMet-sensitive clones by an introduction of a yeast genomic DNA

library are required for the identification of responsible gene. However, null mutants of *met6* (TKY357) and *met17* (TKY358) in SRY5-7 cells did not grow in the presence of 10 mM selenate on SD medium containing 5 μg/ml of methionine (Figure 14B). Since TKY357 (*met6Δ*), but not TKY358 (*met17*Δ), showed a growth defect on SD medium without selenate, I introduced a yeast genomic DNA library into TKY358. Positive screening and color selection on LA-agar medium allowed to isolate some transformants that possessed a plasmid containing *MUP1*. Sequencing of the PCR fragment amplified from SRY5-7 chromosomal DNA revealed a point mutation that changed methionine residue at 74 to isoleucine (ATG changed to ATT) of *MUP1* ORF (*mup1-100*, Figure 15 C and D).

3-4-5. External methionine uptake in *mup1* mutation

S. cerevisiae possesses two methionine specific permease; one is high affinity methionine permease (Mup1p), the other is low affinity methionine permease (Mup3p) (Isnard *et al.* 1996). A deletion of *MUP1* allowed wild-type cells to grow in the presence of SeMet (10 μg/ml), while a deletion of *MUP3* did not show any SeMet resistance (Figure 16A). This result raised the possibility that the SeMet resistance of SRY5-7 may be caused by the inhibition of external SeMet incorporation by high affinity methionine permease Mup1p. On the other hand, the result from microarray analysis indicated that SeMet resistance of *mup1-100* (SRY5-7) might depend on the intracellular level of newly synthesized methionine from sulfate. To address the above issue, I measured the uptake of a radiolabeled methionine into mutant cells. Insnard *et al.* (1996) reported that K_T (K_M of permease) for Mup1p (13μM) is considerably lower than that for Mup3p (1 mM). In order to evaluate the Mup1p activity alone, the uptake

of radiolabeled methionine (20 μM) was measured for 2 min. As shown in Table 8, the uptake rates of external methionine by *mup1*Δ and *mup1*Δ *mup3*Δ cells were very low (1.7–2.6 nmol/min/10^9 cells), while the uptake rate by *mup3*Δ was 69.7 nmol/min/10^9 cells, which was 94% of wild-type level, indicating that the methionine incorporation fully depended on Mup1p under the assay condition. In case of *mup1-100* (SRY5-7) cells, the rate of methionine uptake (13.8 nmol/min/10^9 cells) decreased to 19% of wild-type level. These results indicated that *mup1-100* cells partially impaired the high affinity methionine permease activity. However, it is also known that yeast cells have several kinds of amino acid permeases that show low substrate specificities (Regenberg *et al.* 1999). Thus I further measured the methionine content accumulated in cells with a longer incubation period. When compared the uptake of methionine at 60 min among several strains, the uptake of methionine in *mup1-100* cells was 89% of wild-type level (Figure 16B). In addition, the methionine uptake by *mup1-100* cells was fully recovered to the wild-type level in the presence of 250 μM of methionine under which yeasts are generally cultured (Figure 16C). Since *mup1*Δ *mup3*Δ cells also had an ability to incorporate external methionine into cells at 60% of wild-type level in the presence of 250 μM methionine, it is likely that the *mup1* mutation alone do not inhibit the cellular methionine uptake.

3-5. Discussion

I previously described about the usefulness of *P. pastoris* SMR-94 that shows a resistance to both SeMet and selenate for producing SeMet-labeled proteins suitable for X-ray crystallography. In an effort to identify the genes responsible for the production of proteins containing a high amount of SeMet, I tried to isolate SeMet-resistant *S. cerevisiae* mutant (SRY5-7) that shows a similar phenotype to *P. pastoris* SMR-94 mutant. Each gene deletion of *MET17* and *MET6*, but not of *STR3*, led SRY5-7 cells to lose its SeMet-resistant phenotype (Figure 14A), indicating that SeMet resistance of SRY5-7 mutant depends on an increased methionine pool caused by the overproduction of methionine, as reported for *sam1* mutant (Cherest *et al.* 1973). Although this result remained a possibility that SRY5-7 cells might possess a mutation at a regulatory gene involved in sulfur amino acid, an introduction of a genomic DNA library into TKY358 cells (SRY5-7 cells lacking *MET17* gene) allowed me to isolate a recessive *mup1-100* allele whose methionine residue at position 74 is substituted with isoleucine (Figure 15D).

The methionine uptake assay under the condition that can measure only high affinity methionine permease activity revealed that the rate of methionine uptake by *mup1-100* mutant was significantly lower than that by wild-type cells, while the external methionine was accumulated in *mup1-100* mutant cells with longer incubation or in the presence of 250 μM methionine where yeasts are usually cultured. In addition, the *mup1*Δ *mup3*Δ mutant cells that lack methionine-specific permeases were able to incorporate external methionine when cells were grown in the presence of 250 μM methionine. In *S. cerevisiae*, the uptake of external methionine is mediated by at least

seven permeases, which are Agp1p, Agp3p, Bap2p, Bap3p Gnp1p, Mup3p and Mup1p (Menant *et al.* 2006). For this reason, the methionine uptake by *mup1-100* mutant cells, which partly lack the activity of high affinity permease, will be compensated by the activities from the remaining permeases, providing a reasonable explanation that the *mup1* mutant has an ability to incorporate SeMet into cells.

Since the sulfur amino acid metabolism is regulated at the transcriptional level in *S. cerevisiae* (Thomas and Surdin-Kerjan 1997), DNA microarray analysis was useful to understand the SeMet-resistant mechanism of *mup1* mutant. As compared with wild-type cells, the genes involved in sulfur amino acid metabolism (*MET* genes), especially sulfate assimilation, were significantly up-regulated in *sam1-224* (SRY5-3) and *mup1-100* (SRY5-7) cells. However, when compared between *sam1-224* and *mup1-100* cells, the level of *MET* gene expression was lower in *mup1-100* than in *sam1-224*. These results strongly suggest that *mup1* mutation causes an overproduction of methionine to the extent that the cells can grow in the presence of selenate. Accordingly, *P. pastoris* SMR-94, whose phenotype is similar to *mup1* mutant, could produce SeMet derivative of HLY with a high content of SeMet that are sufficient to determine its crystal structure.

These results not only provide an insight into the SeMet-resistant mechanism of *mup1* mutant but also suggest the potential of *mup1* cells for the production of SeMet-labeled proteins. Since the regulation of sulfur amino acid synthesis is not fully understood, the double screening method by using both SeMet and selenate will enable us to isolate other regulatory mutants that can produce proteins in which SeMet is more efficiently incorporated in future.

GENERAL DISCUSSION

In this thesis, I have developed an expression system to produce recombinant eukaryotic proteins containing SeMet to solve phase problem. For the crystal structural analysis, a large amount of highly purified proteins is required for the screening of protein crystallization. Generally, the target proteins are expressed in *E. coli* that possesses advantages of high productivity and simple culture condition. Thus, most of glycosyltransferases whose crystal structures were solved were expressed in *E. coli* cells. There have been only a few reports on the crystal structure of glycosyltransferase that are overexpressed by eukaryotic cells. These included GnT I (Unligil *et al.* 2000; Gordon *et al.* 2006), ppGalNAcTs (Fritz *et al.* 2004; Fritz *et al.* 2006; Kubota *et al.* 2006), Kre2p/Mnt1p (Lobsanov *et al.* 2004), Fringe (Jinek *et al.* 2006), C2GnT (Pak *et al.* 2006) and Fut8 (Ihara *et al.* 2007). Especially, Kre2/Mnt1 and ppGalNAcTs were overproduced by methylotrophic yeast *P. pastoris* for crystallization. However, the attempt to use *E. coli* for the preparation of recombinant glycosyltransferase has not always been successful. Indeed, α1,6-mannosyltransferase Och1p failed to be expressed as a functional protein (data not shown). In Chapter 1, I purified and characterized recombinant Och1p that was overproduced by *P. pastoris*, indicating that yeast expression system has an advantage for the preparation of recombinant glycosyltransferases that are difficult to produce in *E. coli.*

Even if the target proteins are successfully produced, the problems of crystallization and phase determination still remain. In order to prepare protein crystals, high-throughput crystallization robots may help to search a suitable crystallization condition (Iino *et al.* 2008). The SAD and MAD phasing of SeMet-containing crystals

will provide a solution to the problem of phase determination that can be applied to many kinds of proteins, as compared with either multiple isomorphism replacement or molecular replacement (Ealick 2000). In Chapter 2, I described the isolation of a novel SeMet-resistant mutant (SMR-94) that is resistant to both SeMet and selenate. In addition, I demonstrated that the SMR-94 mutant could produce HLY that contained SeMet at 65% occupancy, which is sufficient to use as a selenomethionine derivative for SAD phasing. These results indicate that *P. pastoris* SMR-94 can contribute to phase determination of eukaryotic proteins including glycosyltransferases that are difficult to be expressed in *E. coli*.

To understand the reason why SeMet-resistant yeast can grow in the presence of SeMet is important for the development of efficient SeMet incorporation system into proteins. In Chapter 3, I characterized SeMet-resistant *S. cerevisiae* mutant (SRY5-7), which showed a similar phenotype to *P. pastoris* SMR-94 that is suitable for SeMet-labeled protein production. I found that SRY5-7 possesses a mutation at *MUP1* gene. I also found that the mutant allele (*mup1-100*) shows the enhanced transcriptional level of *MET* genes, especially those involved in sulfate assimilation pathway. These results suggest that SeMet toxicity is alleviated by the intracellularly overproduced methionine. However, it is noteworthy that the change of *MET* gene transcription in *mup1* mutant was significantly lower than that in *sam1* mutant in which the ability of methionine synthesis is enhanced. Accordingly, *P. pastoris* SMR-94 was assumed to be able to grow in the presence of SeMet and also to produce enough amount of HLY containing SeMet for the phase determination.

Recent report on the SeMet-resistant yeast provided a valuable insight into SeMet toxicity. Malkowski *et al*. (2007) demonstrated that not only *sam1*Δ *sam2*Δ cells

but also *sam1*Δ *sam2*Δ *met6*Δ cells could grow in medium containing SeMet as a sole source of methionine. This result indicates that SeMet toxicity is not due to the incorporation of SeMet into proteins but due to the metabolites synthesized from SeMet. More recent work independently demonstrated that *cys3*Δ mutant, which cannot convert cystathionine to cysteine, is resistant to SeMet, suggesting that the toxic compounds seemed to be selenocysteine or its derivatives converted by the Gsh1p etc. (Figure 7) (Bockhorn *et al.* 2008). On the other hand, I identified selenium atoms around cysteine residues in HLY molecules expressed by *P. pastoris* SMR-94 cells, when an anomalous difference Fourier map was contoured at 5σ (data not shown). This result suggests that SMR-94 has the ability to convert SeMet to selenocysteine and to incorporate selenocysteine into proteins. Thus, it is thought at least that selenocysteine is not a toxic compound for yeast.

For the overproduction of eukaryotic proteins including glycosyltransferase under simple and cost-effective culture conditions, yeasts that show a resistance to both SeMet and selenate have significant advantages over *sam1*Δ *sam2*Δ mutant and *cys3*Δ mutant that require sulfur amino acids for cell proliferation. The SeMet-resistant mutant *P. pastoris* SMR-94 will help to elucidate the molecular mechanism of not only glycosyltransferases but also eukaryotic proteins that are difficult to be overexpressed in *E. coli*.

ACKNOWLEDGEMENTS

I would like to express my sincere gratitude to Dr. Yoshifumi Jigami, Invited Senior Researcher of Research Center for Medical Glycoscience, National Institute of Advanced Industrial Science and Technology (AIST), for his scientific guidance, considerable encouragement and individual discussion that make my research of great achievement and my study life unforgettable.

I would like to express my deepest appreciation to Dr. Satoshi Nishikawa, Deputy Director of Age Dimension Research Center, AIST, for his support and kind guidance throughout the course of this investigation

I am indebted to my committee members, Dr. Yoshihiro Shiraiwa, Dr. Tomoki Chiba, and Dr. Norio Ishida, Graduate School of Life and Environmental Sciences, the University of Tsukuba. I appreciate the major time and effort they all contributed to improve this thesis.

I would like to acknowledge to the continuous guidance and valuable discussions of Dr. Yasunori Chiba, Research Center for Medical Glycoscience, AIST. I wish to express my gratitude to Dr. Hiroto Hirayama, Dr. Morihisa Fujita, Dr. Takuji Oka, Dr, Takehiko Yoko-o, and Dr. Yoh-ichi Shimma, group members of our laboratory, for their experimental guidance and helpful discussions.

I am grateful to Dr. Tomomi Kubota, Research Center for Medical Glycoscience, AIST, for his scientific and technological support in X-ray structural analysis (Chapter 1 & 2).

I am grateful to Dr. Hiroki Shimizu, Drug-Seeds Discovery Research Laboratory, AIST, for providing Man-α1,2-Man-α1,3-Man tri-saccharides (Chapter 1).

I am grateful to Mr. Satoshi Kondou, New Projects Development Division, Toray Industries Inc., for technological support in microarray analysis (Chapter 3).

Finally, I would like to deeply thank my families and my friends for their continuous encouragement, understanding and support throughout my study.

Toshihiko Kitajima

Tsukuba, January 2009

REFERENCES

Ballou, C. E., L. Ballou and G. Ball (1994). *Schizosaccharomyces pombe* glycosylation mutant with altered cell surface properties. *Proc Natl Acad Sci U S A* **91**: 9327-9331.

Barnay-Verdier, S., A. Boisrame and J. M. Beckerich (2004). Identification and characterization of two alpha-1,6-mannosyltransferases, Anl1p and Och1p, in the yeast *Yarrowia lipolytica*. *Microbiology* **150**: 2185-2195.

Barton, W. A., D. Tzvetkova-Robev, H. Erdjument-Bromage, P. Tempst and D. B. Nikolov (2006). Highly efficient selenomethionine labeling of recombinant proteins produced in mammalian cells. *Protein Sci* **15**: 2008-2013.

Bockhorn, J., B. Balar, D. He, E. Seitomer, P. R. Copeland and T. G. Kinzy (2008). Genome-wide screen of *Saccharomyces cerevisiae* null allele strains identifies genes involved in selenomethionine resistance. *Proc Natl Acad Sci U S A* **105**: 17682-17687.

Breton, C., E. Bettler, D. H. Joziasse, R. A. Geremia and A. Imberty (1998). Sequence-function relationships of prokaryotic and eukaryotic galactosyltransferases. *J Biochem* **123**: 1000-1009.

Breton, C. and A. Imberty (1999). Structure/function studies of glycosyltransferases. *Current Opinion in Structural Biology* **9**: 563-571.

Bushnell, D. A., P. Cramer and R. D. Kornberg (2001). Selenomethionine incorporation in *Saccharomyces cerevisiae* RNA polymerase II. *Structure* **9**: R11-14.

Byrd, J. C., A. L. Tarentino, F. Maley, P. H. Atkinson and R. B. Trimble (1982). Glycoprotein synthesis in yeast. Identification of $Man_8GlcNAc_2$ as an essential

intermediate in oligosaccharide processing. *J Biol Chem* **257**: 14657-14666.

Cantarel, B. L., P. M. Coutinho, C. Rancurel, T. Bernard, V. Lombard and B. Henrissat (2008). The Carbohydrate-Active EnZymes database (CAZy): an expert resource for Glycogenomics. *Nucleic Acids Research.*

CCP4 [Collaborative Computational Project, Number 4] (1994). The CCP4 suite: programs for protein crystallography. *Acta Crystallogr D Biol Crystallogr.* **50**(Pt 5)**:** 760-763.

Charnock, S. J. and G. J. Davies (1999). Structure of the nucleotide-diphospho-sugar transferase, SpsA from *Bacillus subtilis*, in native and nucleotide-complexed forms. *Biochemistry* **38**: 6380-6385.

Cherest, H. and Y. Surdin-Kerjan (1981). The two methionine adenosyl transferases in *Saccharomyces cerevisiae*: evidence for the existence of dimeric enzymes. *Mol Gen Genet* **182**: 65-69.

Cherest, H., Y. Surdin-Kerjan, J. Antoniewski and H. de Robichon-Szulmajster (1973). Effects of regulatory mutations upon methionine biosynthesis in *Saccharomyces cerevisiae*: loci *eth2-eth3-eth10*. *J Bacteriol* **115**: 1084-1093.

Cowtan, K. (1994). DM: An automated procedure for phase improvement by density modification. *Joint CCP4 and ESF-EACBM Newsletter on Protein Crystallography* **31**: 34-38.

Cregg, J. M., K. Madden, G. P. Thill and C. A. Stillman (1989). Functional characterization of the two alcohol oxidase genes from the yeast *Pichia pastoris.* *Mol Cell Biol* **9**: 1316-1323.

Cregg, J. M., T. S. Vedvick and W. C. Raschke (1993). Recent advances in the expression of foreign genes in *Pichia pastoris*. *Biotechnology (N Y)* **11**:

905-910.

Cronin, C. N., K. B. Lim and J. Rogers (2007). Production of selenomethionyl-derivatized proteins in baculovirus-infected insect cells. *Protein Science* **16**: 2023-2029.

Davis, S. J., S. Ikemizu, A. V. Collins, J. A. Fennelly, K. Harlos, E. Y. Jones and D. I. Stuart (2001). Crystallization and functional analysis of a soluble deglycosylated form of the human costimulatory molecule B7-1. *Acta Crystallogr D Biol Crystallogr* **57**: 605-608.

Dean, N. (1999). Asparagine-linked glycosylation in the yeast Golgi. *Biochim Biophys Acta* **1426**: 309-322.

Despreaux, C. W. and R. F. Manning (1993). The *dacA* gene of *Bacillus stearothermophilus* coding for D-alanine carboxypeptidase: cloning, structure and expression in *Escherichia coli* and *Pichia pastoris*. *Gene* **131**: 35-41.

Ealick, S. E. (2000). Advances in multiple wavelength anomalous diffraction crystallography. *Current Opinion in Chemical Biology* **4**: 495-499.

Emsley, P. and K. Cowtan (2004). Coot: model-building tools for molecular graphics. *Acta Crystallogr D Biol Crystallogr* **60**: 2126-2132.

Fritz, T. A., J. H. Hurley, L. B. Trinh, J. Shiloach and L. A. Tabak (2004). The beginnings of mucin biosynthesis: the crystal structure of UDP-GalNAc:polypeptide alpha-*N*-acetylgalactosaminyltransferase-T1. *Proceedings of the National Academy of Sciences of the United States of America* **101**: 15307-15312.

Fritz, T. A., J. Raman and L. A. Tabak (2006). Dynamic association between the catalytic and lectin domains of human UDP-GalNAc:polypeptide

alpha-*N*-acetylgalactosaminyltransferase-2. *Journal of Biological Chemistry* **281**: 8613-8619.

Gaynor, E. C., S. te Heesen, T. R. Graham, M. Aebi and S. D. Emr (1994). Signal-mediated retrieval of a membrane protein from the Golgi to the ER in yeast. *J Cell Biol* **127**: 653-665.

Gemmill, T. R. and R. B. Trimble (1999). Overview of *N*- and *O*-linked oligosaccharide structures found in various yeast species. *Biochim Biophys Acta* **1426**: 227-237.

Gietz, R. D., R. H. Schiestl, A. R. Willems and R. A. Woods (1995). Studies on the transformation of intact yeast cells by the LiAc/SS-DNA/PEG procedure. *Yeast* **11**: 355-360.

Gordon, R. D., P. Sivarajah, M. Satkunarajah, D. Ma, C. A. Tarling, D. Vizitiu, S. G. Withers and J. M. Rini (2006). X-ray crystal structures of rabbit *N*-acetylglucosaminyltransferase I (GnT I) in complex with donor substrate analogues. *Journal of Molecular Biology* **360**: 67-79.

Hanahan, D. (1983). Studies on transformation of *Escherichia coli* with plasmids. *J Mol Biol* **166**: 557-580.

Helenius, A. and M. Aebi (2001). Intracellular functions of *N*-linked glycans. *Science* **291**: 2364-2369.

Hendrickson, W. A., J. R. Horton and D. M. LeMaster (1990). Selenomethionyl proteins produced for analysis by multiwavelength anomalous diffraction (MAD): a vehicle for direct determination of three-dimensional structure. *EMBO Journal* **9**: 1665-1672.

Herscovics, A. (1999). Processing glycosidases of *Saccharomyces cerevisiae. Biochim Biophys Acta* **1426**: 275-285.

Ihara, H., Y. Ikeda, S. Toma, X. Wang, T. Suzuki, J. Gu, E. Miyoshi, T. Tsukihara, K. Honke, A. Matsumoto, A. Nakagawa and N. Taniguchi (2007). Crystal structure of mammalian alpha1,6-fucosyltransferase, FUT8. *Glycobiology* **17**: 455-466.

Iino, H., H. Naitow, Y. Nakamura, N. Nakagawa, Y. Agari, M. Kanagawa, A. Ebihara, A. Shinkai, M. Sugahara, M. Miyano, N. Kamiya, S. Yokoyama, K. Hirotsu and S. Kuramitsu (2008). Crystallization screening test for the whole-cell project on *Thermus thermophilus* HB8. *Acta Crystallogr Sect F Struct Biol Cryst Commun* **64**: 487-491.

Inaka, K., Y. Taniyama, M. Kikuchi, K. Morikawa and M. Matsushima (1991). The crystal structure of a mutant human lysozyme C77/95A with increased secretion efficiency in yeast. *J Biol Chem* **266**: 12599-12603.

Isnard, A. D., D. Thomas and Y. Surdin-Kerjan (1996). The study of methionine uptake in *Saccharomyces cerevisiae reveals* a new family of amino acid permeases. *J Mol Biol* **262**: 473-484.

Jinek, M., Y. W. Chen, H. Clausen, S. M. Cohen and E. Conti (2006). Structural insights into the Notch-modifying glycosyltransferase Fringe. *Nature Structural and Molecular Biology* **13**: 945-946.

Jungmann, J. and S. Munro (1998). Multi-protein complexes in the cis Golgi of *Saccharomyces cerevisiae* with alpha-1,6-mannosyltransferase activity. *Embo J* **17**: 423-434.

Jungmann, J., J. C. Rayner and S. Munro (1999). The *Saccharomyces cerevisiae* protein Mnn10p/Bed1p is a subunit of a Golgi mannosyltransferase complex. *J Biol Chem* **274**: 6579-6585.

Kawasaki, T. (2003). Glycobiology basics: glycoproteins. *Tanpakushitsu Kakusan Koso*

48: 910-915.

Kubota, T., T. Shiba, S. Sugioka, S. Furukawa, H. Sawaki, R. Kato, S. Wakatsuki and H. Narimatsu (2006). Structural basis of carbohydrate transfer activity by human UDP-GalNAc: polypeptide alpha-*N*-acetylgalactosaminyltransferase (pp-GalNAc-T10). *Journal of Molecular Biology* **359**: 708-727.

Kuras, L., A. Rouillon, T. Lee, R. Barbey, M. Tyers and D. Thomas (2002). Dual regulation of the met4 transcription factor by ubiquitin-dependent degradation and inhibition of promoter recruitment. *Mol Cell* **10**: 69-80.

Laemmli, U. K. (1970). Cleavage of structural proteins during the assembly of the head of bacteriophage T4. *Nature* **227**: 680-685.

Larsson, A. M., J. Ståhlberg and T. A. Jones (2002). Preparation and crystallization of selenomethionyl dextranase from *Penicillium minioluteum* expressed in *Pichia pastoris*. *Acta Crystallogr D Biol Crystallogr* **58**: 346-348.

Laurila, M. R., P. S. Salgado, E. V. Makeyev, J. Nettelship, D. I. Stuart, J. M. Grimes and D. H. Bamford (2005). Gene silencing pathway RNA-dependent RNA polymerase of *Neurospora crassa*: yeast expression and crystallization of selenomethionated QDE-1 protein. *J Struct Biol* **149**: 111-115.

Lobsanov, Y. D., P. A. Romero, B. Sleno, B. Yu, P. Yip, A. Herscovics and P. L. Howell (2004). Structure of Kre2p/Mnt1p: a yeast alpha1,2-mannosyltransferase involved in mannoprotein biosynthesis. *J Biol Chem* **279**: 17921-17931.

Longtine, M. S., A. McKenzie, 3rd, D. J. Demarini, N. G. Shah, A. Wach, A. Brachat, P. Philippsen and J. R. Pringle (1998). Additional modules for versatile and economical PCR-based gene deletion and modification in *Saccharomyces cerevisiae*. *Yeast* **14**: 953-961.

Lustbader, J. W., H. Wu, S. Birken, S. Pollak, M. A. Gawinowicz Kolks, A. M. Pound, D. Austen, W. A. Hendrickson and R. E. Canfield (1995). The expression, characterization, and crystallization of wild-type and selenomethionyl human chorionic gonadotropin. *Endocrinology* **136**: 640-650.

Malkowski, M. G., E. Quartley, A. E. Friedman, J. Babulski, Y. Kon, J. Wolfley, M. Said, J. R. Luft, E. M. Phizicky, G. T. DeTitta and E. J. Grayhack (2007). Blocking *S*-adenosylmethionine synthesis in yeast allows selenomethionine incorporation and multiwavelength anomalous dispersion phasing. *Proceedings of the National Academy of Sciences of the United States of America* **104**: 6678-6683.

Menant, A., R. Barbey and D. Thomas (2006). Substrate-mediated remodeling of methionine transport by multiple ubiquitin-dependent mechanisms in yeast cells. *Embo J* **25**: 4436-4447.

Movsichoff, F., O. A. Castro and A. J. Parodi (2005). Characterization of *Schizosaccharomyces pombe* ER alpha-mannosidase: a reevaluation of the role of the enzyme on ER-associated degradation. *Mol Biol Cell* **16**: 4714-4724.

Murshudov, G. N., A. A. Vagin and E. J. Dodson (1997). Refinement of macromolecular structures by the maximum-likelihood method. *Acta Crystallogr D Biol Crystallogr* **53**: 240-255.

Nakanishi-Shindo, Y., K. Nakayama, A. Tanaka, Y. Toda and Y. Jigami (1993). Structure of the *N*-linked oligosaccharides that show the complete loss of alpha-1,6-polymannose outer chain from *och1*, *och1 mnn1*, and *och1 mnn1 alg3* mutants of *Saccharomyces cerevisiae. J Biol Chem* **268**: 26338-26345.

Nakayama, K., T. Nagasu, Y. Shimma, J. Kuromitsu and Y. Jigami (1992). *OCH1*

encodes a novel membrane bound mannosyltransferase: outer chain elongation of asparagine-linked oligosaccharides. *Embo J* **11**: 2511-2519.

Nakayama, K., Y. Nakanishi-Shindo, A. Tanaka, Y. Haga-Toda and Y. Jigami (1997). Substrate specificity of alpha-1,6-mannosyltransferase that initiates *N*-linked mannose outer chain elongation in *Saccharomyces cerevisiae. FEBS Lett* **412**: 547-550.

Nishihara, S., H. Iwasaki, M. Kaneko, A. Tawada, M. Ito and H. Narimatsu (1999). Alpha1,3-fucosyltransferase 9 (FUT9; Fuc-TIX) preferentially fucosylates the distal GlcNAc residue of polylactosamine chain while the other four alpha1,3FUT members preferentially fucosylate the inner GlcNAc residue. *FEBS Lett* **462**: 289-294.

Ono, B., N. Ishii, S. Fujino and I. Aoyama (1991). Role of hydrosulfide ions (HS-) in methylmercury resistance in *Saccharomyces cerevisiae. Appl Environ Microbiol* **57**: 3183-3186.

Otwinowski, Z. and W. Minor (1997). Processing of X-ray diffraction data collected in oscillation mode. *Methods in Enzymology* **276**: 307-326.

Pak, J. E., P. Arnoux, S. Zhou, P. Sivarajah, M. Satkunarajah, X. Xing and J. M. Rini (2006). X-ray crystal structure of leukocyte type core 2 beta1,6-*N*-acetylglucosaminyltransferase. Evidence for a convergence of metal ion-independent glycosyltransferase mechanism. *Journal of Biological Chemistry* **281**: 26693-26701.

Perrakis, A., R. Morris and V. S. Lamzin (1999). Automated protein model building combined with iterative structure refinement. *Nat Struct Biol* **6**: 458-463.

Persson, K., H. D. Ly, M. Dieckelmann, W. W. Wakarchuk, S. G. Withers and N. C.

Strynadka (2001). Crystal structure of the retaining galactosyltransferase LgtC from *Neisseria meningitidis* in complex with donor and acceptor sugar analogs. *Nature Structural Biology* **8**: 166-175.

Puccia, R., B. Grondin and A. Herscovics (1993). Disruption of the processing alpha-mannosidase gene does not prevent outer chain synthesis in *Saccharomyces cerevisiae. Biochem J* **290 (Pt 1)**: 21-26.

Rayner, J. C. and S. Munro (1998). Identification of the *MNN2* and *MNN5* mannosyltransferases required for forming and extending the mannose branches of the outer chain mannans of *Saccharomyces cerevisiae. J Biol Chem* **273**: 26836-26843.

Regenberg, B., L. During-Olsen, M. C. Kielland-Brandt and S. Holmberg (1999). Substrate specificity and gene expression of the amino-acid permeases in *Saccharomyces cerevisiae. Curr Genet* **36**: 317-328.

Rice, L. M., T. N. Earnest and A. T. Brunger (2000). Single-wavelength anomalous diffraction phasing revisited. *Acta Crystallogr D Biol Crystallogr* **56**: 1413-1420.

Romero, P. A., M. Lussier, A. M. Sdicu, H. Bussey and A. Herscovics (1997). Ktr1p is an alpha-1,2-mannosyltransferase of *Saccharomyces cerevisiae.* Comparison of the enzymic properties of soluble recombinant Ktr1p and Kre2p/Mnt1p produced in *Pichia pastoris. Biochem J* **321 (Pt 2)**: 289-295.

Schrauzer, G. N. (2003). The nutritional significance, metabolism and toxicology of selenomethionine. *Advances in Food and Nutrition Research* **47**: 73-112.

Scorer, C. A., R. G. Buckholz, J. J. Clare and M. A. Romanos (1993). The intracellular production and secretion of HIV-1 envelope protein in the methylotrophic yeast

Pichia pastoris. Gene **136**: 111-119.

Sheldrick, G. M. (2008). A short history of SHELX. *Acta Crystallogr A Found Crystallogr* **64**: 112-122.

Sinnott, M. L. (1990). Catalytic mechanism of enzymic glycosyl transfer. *Chemical Reviews* **90**: 1171-1202.

Sutton, A., D. Immanuel and K. T. Arndt (1991). The *SIT4* protein phosphatase functions in late G1 for progression into S phase. *Mol Cell Biol* **11**: 2133-2148.

Tarbouriech, N., S. J. Charnock and G. J. Davies (2001). Three-dimensional structures of the Mn and Mg dTDP complexes of the family GT-2 glycosyltransferase SpsA: a comparison with related NDP-sugar glycosyltransferases. *Journal of Molecular Biology* **314**: 655-661.

Thomas, D. and Y. Surdin-Kerjan (1997). Metabolism of sulfur amino acids in *Saccharomyces cerevisiae. Microbiol Mol Biol Rev* **61**: 503-532.

Thomson, L. M., S. Bates, S. Yamazaki, M. Arisawa, Y. Aoki and N. A. Gow (2000). Functional characterization of the *Candida albicans MNT1* mannosyltransferase expressed heterologously in *Pichia pastoris. J Biol Chem* **275**: 18933-18938.

Unligil, U. M., S. Zhou, S. Yuwaraj, M. Sarkar, H. Schachter and J. M. Rini (2000). X-ray crystal structure of rabbit *N*-acetylglucosaminyltransferase I: catalytic mechanism and a new protein superfamily. *EMBO Journal* **19**: 5269-5280.

Vrielink, A., W. Ruger, H. P. Driessen and P. S. Freemont (1994). Crystal structure of the DNA modifying enzyme beta-glucosyltransferase in the presence and absence of the substrate uridine diphosphoglucose. *EMBO Journal* **13**: 3413-3422.

Wiggins, C. A. and S. Munro (1998). Activity of the yeast *MNN1*

alpha-1,3-mannosyltransferase requires a motif conserved in many other families of glycosyltransferases. *Proc Natl Acad Sci U S A* **95**: 7945-7950.

Wu, M. M., M. Grabe, S. Adams, R. Y. Tsien, H. P. Moore and T. E. Machen (2001). Mechanisms of pH regulation in the regulated secretory pathway. *J Biol Chem* **276**: 33027-33035.

Xu, B., I. G. Muñoz I, J. C. Janson and J. Ståhlberg (2002). Crystallization and X-ray analysis of native and selenomethionyl beta-mannanase Man5A from blue mussel, *Mytilus edulis*, expressed in *Pichia pastoris*. *Acta Crystallogr D Biol Crystallogr* **58**: 542-545.

Yip, C. L., S. K. Welch, F. Klebl, T. Gilbert, P. Seidel, F. J. Grant, P. J. O'Hara and V. L. MacKay (1994). Cloning and analysis of the *Saccharomyces cerevisiae MNN9* and *MNN1* genes required for complex glycosylation of secreted proteins. *Proc Natl Acad Sci U S A* **91**: 2723-2727.

Yoko-o, T., K. Tsukahara, T. Watanabe, N. Hata-Sugi, K. Yoshimatsu, T. Nagasu and Y. Jigami (2001). *Schizosaccharomyces pombe och1*$^{+}$ encodes alpha-1,6-mannosyltransferase that is involved in outer chain elongation of *N*-linked oligosaccharides. *FEBS Lett* **489**: 75-80.

Ziegler, F. D., T. R. Gemmill and R. B. Trimble (1994). Glycoprotein synthesis in yeast. Early events in N-linked oligosaccharide processing in *Schizosaccharomyces pombe*. *J Biol Chem* **269**: 12527-12535.

FIGURES AND TABLES

Table 1. *S. cerevisiae* strains used in this study.

Table 2. Substrate specificity of the recombinant Och1p.

Table 3. Effects of divalent metal ions and EDTA on the Och1p activity.

Table 4. Amino acid composition of native and selenomethionyl HLY.

Table 5. Overview of differently expressed genes in SeMet-resistant mutants.

Table 6. Genes up-regulated above 3-fold in SRY5-3.

Table 7. Genes up-regulated above 3-fold in SRY5-7.

Table 8. Rates of methionine uptake in different strains.

Figure 1. Expression construct and analysis of purified protein by SDS- PAGE.

Figure 2. Structures of pyridylaminated oligosaccharides used as acceptors in this study.

Figure 3. The novel product obtained from $Man_9GlcNAc_2$-PA by recombinant Och1p.

Figure 4. Confirmation of the structure of the novel product generated by recombinant Och1p.

Figure 5. Effects of acceptor structure on the incorporation of an additional mannose by recombinant Och1p.

Figure 6. Positions of the first and second mannose additions to the M6C substrate.

Figure 7. Metabolic pathway of sulfur compounds in *S. cerevisiae.*

Figure 8. Comparison of productivity with promoters to produce recombinant HLY protein in synthetic complete medium.

Figure 9. Growth phenotype of *P. pastoris* SMR mutants.

Figure 10. Peptide mass analyses of selenomethionyl HLY proteins.

Figure 11. Stereoview of electron density maps in the region of 16-Gly, 17-Met, 18-Asp, 28-Trp, 29-Met, 30-Cys and 31-Leu.

Figure 12. Growth phenotype of SeMet-resistant mutants.

Figure 13. Comparison of level of gene expression in each SeMet-resistant mutant.

Figure 14. Alteration of phenotypes of SeMet-resistant mutants by the blocking of methionine synthesis.

Figure 15. Complementation of SeMet-resistant mutants.

Figure 16. Effect of the mutation of genes encoding methionine permease on SeMet resistance and methionine uptake.

Table 1. *S. cerevisiae* strains used in this study.

Strain	Harboring plasmid	Genotype	Source
W303-1A		*MAT***a** *leu2-3,112 his3-11 ade2-1 ura3-1 trp1-1 can1-100*	Sutton et al., 1991
W303-1B		*MATa leu2-3,112 his3-11 ade2-1 ura3-1 trp1-1 can1-100*	Sutton et al., 1991
SRY5-3		*MAT***a** *sam1-224 W303*	This study
SRY5-7		*MAT***a** *mup1-100 W303*	This study
TKY300	pRS316	*MAT***a** *W303*	This study
TKY302	pRS316	*MAT***a** *SRY5-3*	This study
TKY303	pRS316	*MAT***a** *SRY5-7*	This study
TKY343		*MAT***a** *met6Δ::His3MX6 W303*	This study
TKY350		*MAT***a** *met17Δ::His3MX6 W303*	This study
TKY354		*MAT***a** *met6Δ::His3MX6 SRY5-3*	This study
TKY355		*MAT***a** *met17Δ::His3MX6 SRY5-3*	This study
TKY357		*MAT***a** *met6Δ::His3MX6 SRY5-7*	This study
TKY358		*MAT***a** *met17Δ::His3MX6 SRY5-7*	This study
TKY359		*MAT***a** *str3Δ::His3MX6 W303*	This study
TKY360		*MAT***a** *str3Δ::His3MX6 SRY5-3*	This study
TKY361		*MAT***a** *str3Δ::His3MX6 SRY5-7*	This study
TKY364	pRS316-SAM1	*MAT***a** *SRY5-3*	This study
TKY385	pRS316-MUP1	*MAT***a** *SRY5-7*	This study
TKY386		*MAT***a** *mup1Δ::His3MX6 W303*	This study
TKY387		*MAT***a** *mup3Δ::His3MX6 W303*	This study
TKY388		*MAT***a** *mup1Δ::TRP1 mup3Δ::His3MX6 W303*	This study

Table 2. Substrate specificity of the recombinant Och1p.

Acceptor	Relative activity (%)	
	Recombinant Och1p[a]	Microsomal fraction[b]
M9A	74.2	84.7
M8A	100	100
M8B	54.5	58.5
M8C	27	28.8
M7A	60.4	66.1
M7B	25.2	28.8
M7D	13.8	14.4
M6B	15.9	14.4
M6C	0	0
M5A	0	0

[a] The enzymatic reaction was carried out using 1.36 μg/ml of Och1p.

[b] The values were previously reported by Yoko-o *et al.* (1999).

Table 3. Effects of divalent metal ions and EDTA on the Och1p activity.

Metal salt[a]	Specific activity[b] (nmol/mg protein/min)
None	0
$MnCl_2$	95
$MgCl_2$	0
$CaCl_2$	0
$CoCl_2$	8
$NiCl_2$	0
$CuCl_2$	0
$ZnCl_2$	0
$CdCl_2$	4

[a]The enzymatic reaction was carried out by using 0.54 μg/ml of Och1p and various divalent cation chlorides at the final concentration of 10 mM.

[b]To remove the trace amount of cations, the stock Och1p solution was diluted with 50 mM Tris-HCl, pH 7.5, containing 10 mM EDTA and the reaction.

Table 4. Amino acid composition of native and selenomethionyl HLY.

	Theoretical	SMD1168[a]		SMR-94[b]	
	mol%	mol%	ratio	mol%	ratio
Met	1.7	1.6	0.9	0.6	0.3
Ala	12.2	12.1	1.0	12.5	1.0
Arg	12.2	11.9	1.0	12.3	1.0
Asn+Asp	15.7	15.0	1.0	16.0	1.0
Gln+Glu	8.7	9.3	1.1	9.0	1.0
Gly	9.6	9.5	1.0	10.1	1.1
His	0.0	0.3	-	0.0	-
Ile	4.3	4.2	1.0	4.4	1.0
Leu	7.0	6.8	1.0	7.2	1.0
Lys	4.3	6.2	1.4	4.7	1.1
Phe	1.7	1.7	1.0	1.6	0.9
Ser	5.2	5.0	1.0	4.8	0.9
Thr	4.3	4.3	1.0	4.4	1.0
Tyr	5.2	4.9	0.9	4.9	0.9
Val	7.8	7.2	0.9	7.5	1.0

Values are expressed as mol% and the ratio of experimental values to theoretical values. Cys and Trp were omitted due to degradation during acid hydrolysis. Pro also was omitted because its ninhydrin derivative showed low sensitivity.

[a]HLY was expressed by SMD1168 cells in the presence of 50 μg/ml Met.

[b]HLY was expressed by SMR-94 cells in the presence of 50 μg/ml SeMet.

Table 5. Overview of differently expressed genes in SeMet-resistant mutants.

	SRY5-7	SRY5-3
Down-regurated gene (<0.33)	248	223
Up-regulated gene (3<)	17	61
Categories for upregulated genes		
Sulfate assimilation	4	7
Met and AdoMet biosynthesis	2	2
Sulfide incorporation and trans sulfuration	1	4
Sulfur compound uptake	2	4
MET gene's regulation	1	1
Others	5	30
Unknown	2	13

Table 6. Genes up-regulated above 3-fold in SRY5-3.

ORF name	Gene name	Fold change	Descriptions
YBR294W	*SUL1*	273.3	High affinity sulfate permease
YLL055W	*YCT1*	34.2	High-affinity cysteine-specific transporter
YLR092W	*SUL2*	24.7	High affinity sulfate permease
YLL057C	*JLP1*	22.7	Fe(II)-dependent sulfonate/α-ketoglutarate dioxygenase
YGL125W	*MET13*	20.5	Major isozyme of methylenetetrahydrofolate reductase
YJR010W	*MET3*	19.5	ATP sulfurylase
YKL001C	*MET14*	17.6	Adenylylsulfate kinase
YAL067C	*SEO1*	17.5	Putative permease
YER091C	*MET6*	17.4	Cobalamin-independent methionine synthase
YOL164W	*BDS1*	13.7	Bacterially-derived sulfatase
YGR087C	*PDC6*	13.2	Minor isoform of pyruvate decarboxylase
YIR017C	*MET28*	12.0	Basic leucine zipper transcriptional activator
YKR069W	*MET1*	11.1	*S*-adenosyl-L-methionine uroporphyrinogen III transmethylase
YHR176W	*FMO1*	11.1	Flavin-containing monooxygenase
YFR030W	*MET10*	10.2	Subunit alpha of assimilatory sulfite reductase
YIL164C	*NIT1*	9.5	Nitrilase
YDL059C	*RAD59*	8.2	Protein involved in the repair of double-strand breaks in DNA
YFL055W	*AGP3*	8.2	Low-affinity amino acid permease
YLR303W	*MET17*	7.9	*O*-acetyl homoserine sulfhydrylase
YBR213W	*MET8*	7.4	Bifunctional dehydrogenase and ferrochelatase
YIL165C	—	7.4	Putative protein of unknown function
YNL277W	*MET2*	6.8	L-homoserine-*O*-acetyltransferase
YPR167C	*MET16*	6.3	3'-phosphoadenylsulfate reductase
YJR137C	*ECM17*	6.0	Sulfite reductase beta subunit
YPL250C	*ICY2*	5.4	Protein of unknown function
YGL184C	*STR3*	5.4	Cystathionine β-lyase
YOL162W	—	5.3	Putative protein of unknown function
YLR364W	*GRX8*	5.3	Putative cytosolic dithiol glutaredoxin
YLL052C	*AQY2*	4.8	Water channel
YLL061W	*MMP1*	4.5	High-affinity *S*-methylmethionine permease
YOL163W	—	4.4	Putative protein of unknown function
YCL026C-B	*HBN1*	4.4	Putative protein of unknown function
YML116W	*ATR1*	4.4	Multidrug efflux pump of the major facilitator superfamily
YAL012W	*CYS3*	4.4	Cystathionine γ-lyase

Table 6. Continued

ORF name	Gene name	Fold change	Descriptions
YIL074C	*SER33*	4.1	3-phosphoglycerate dehydrogenase
YMR120C	*ADE17*	4.1	Enzyme of '*de novo*' purine biosynthesis
YLR058C	*SHM2*	4.1	Cytosolic serine hydroxymethyltransferase
YNL241C	*ZWF1*	4.0	Glucose-6-phosphate dehydrogenase
YDL198C	*GGC1*	4.0	Mitochondrial GTP/GDP transporter
YMR189W	*GCV2*	4.0	P subunit of the mitochondrial glycine decarboxylase complex
YJL212C	*OPT1*	3.9	Proton-coupled oligopeptide transporter of the plasma membrane
YBR147W	*RTC2*	3.8	Protein of unknown function
YPR194C	*OPT2*	3.8	Oligopeptide transporter; member of the OPT family
YLL053C	—	3.7	Putative protein
YBR011C	*IPP1*	3.6	Cytoplasmic inorganic pyrophosphatase
YHR183W	*GND1*	3.6	6-phosphogluconate dehydrogenase
YOR009W	*TIR4*	3.4	Cell wall mannoprotein
YOL158C	*ENB1*	3.4	Endosomal ferric enterobactin transporter
YOR130C	*ORT1*	3.4	Ornithine transporter of the mitochondrial inner membrane
YJL079C	*PRY1*	3.4	Protein of unknown function
YLR089C	*ALT1*	3.4	Putative alanine transaminase
YGR254W	*ENO1*	3.3	Enolase I
YOL013W-B	—	3.3	Dubious open reading frame unlikely to encode a protein
YOR303W	*CPA1*	3.2	Small subunit of carbamoyl phosphate synthetase
YLR154W-E	—	3.2	Dubious open reading frame unlikely to encode a protein
YER145C	*FTR1*	3.2	High affinity iron permease
YIR019C	*MUC1*	3.2	GPI-anchored cell surface glycoprotein
YLL058W	—	3.1	Putative protein of unknown function
YHL036W	*MUP3*	3.1	Low affinity methionine permease
YJL060W	*BNA3*	3.1	Kynurenine aminotransferase
YOR378W	—	3.0	Putative protein of unknown function

Table 7. Genes up-regulated above 3-fold in SRY5-7.

ORF name	Gene name	Fold change	Descriptions
YBR294W	*SUL1*	17.9	High affinity sulfate permease
YLR092W	*SUL2*	6.7	High affinity sulfate permease
YKL001C	*MET14*	6.1	Adenylylsulfate kinase
YJR010W	*MET3*	6.0	ATP sulfurylase
YAL067C	*SEO1*	4.4	Putative permease
YKR069W	*MET1*	4.3	*S*-adenosyl-L-methionine uroporphyrinogen III transmethylase
YFR030W	*MET10*	4.1	Subunit alpha of assimilatory sulfite reductase
YER091C	*MET6*	3.9	Cobalamin-independent methionine synthase
YLR154C-G	—	3.5	Putative protein of unknown function
YGL125W	*MET13*	3.4	Major isozyme of methylenetetrahydrofolate reductase
YLL055W	*YCT1*	3.2	High-affinity cysteine-specific transporter
YDL059C	*RAD59*	3.2	Protein involved in the repair of double-strand breaks in DNA
YLR154W-E	—	3.2	Dubious open reading frame unlikely to encode a protein
YIR017C	*MET28*	3.2	Basic leucine zipper transcriptional activator
YLR154W-C	*TAR1*	3.1	Mitochondrial protein potentially involved in regulation of respiratory
YGL184C	*STR3*	3.0	Cystathionine β-lyase
YDR233C	*RTN1*	3.0	ER membrane protein

Table 8. Rates of methionine uptake in different strains.

Strain	Rate[a] (nmol/min/10^9cells)
Wild-type	74.5 ± 15.6
SRY5-7 (*mup1-100*)	13.8 ± 1.0
*mup1*Δ	2.6 ± 0.7
*mup3*Δ	69.7 ± 5.5
*mup1*Δ*mup3*Δ	1.7 ± 0.4

[a]Methionine uptake was measured for two minutes at 20 mM of [methyl-^{3}H] methionine. Values are the average ± standard deviation of three assays.

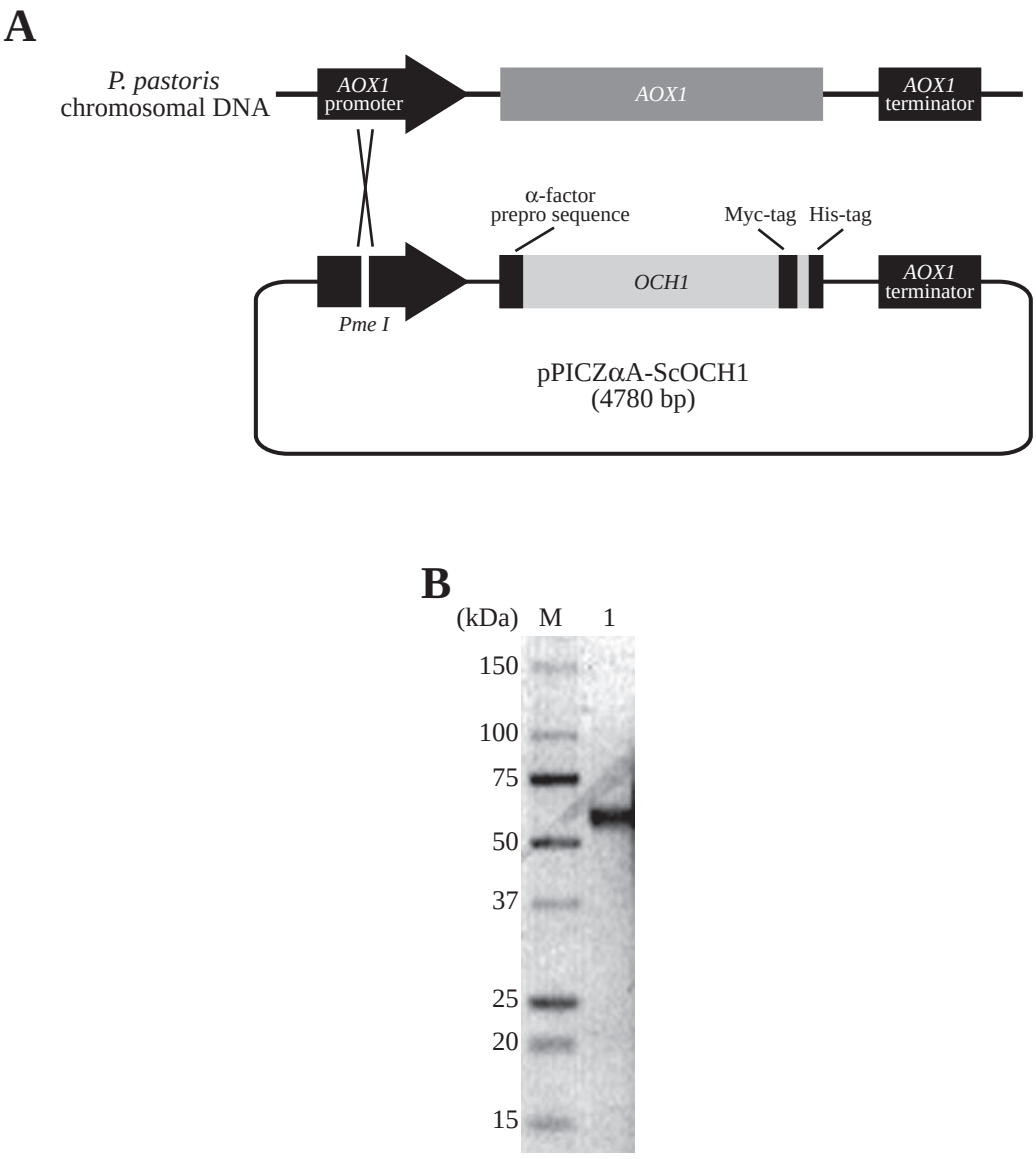

Figure 1. Expression construct and analysis of purified protein by SDS-PAGE. *A,* the structure of the expression plasmid and the scheme of integration into *P. pastoris* chromosomal DNA are shown. *Pme*I and crossover mean homologous recombination at the *PmeI* site. ***B,*** after the purification of recombinant Och1p from the culture supernatant, the sample was analyzed by SDS-PAGE (5–20% gradient gel; ATTO, Tokyo, Japan). Lane M; molecular weight marker (Bio-Rad), lane 1; purified Och1p.

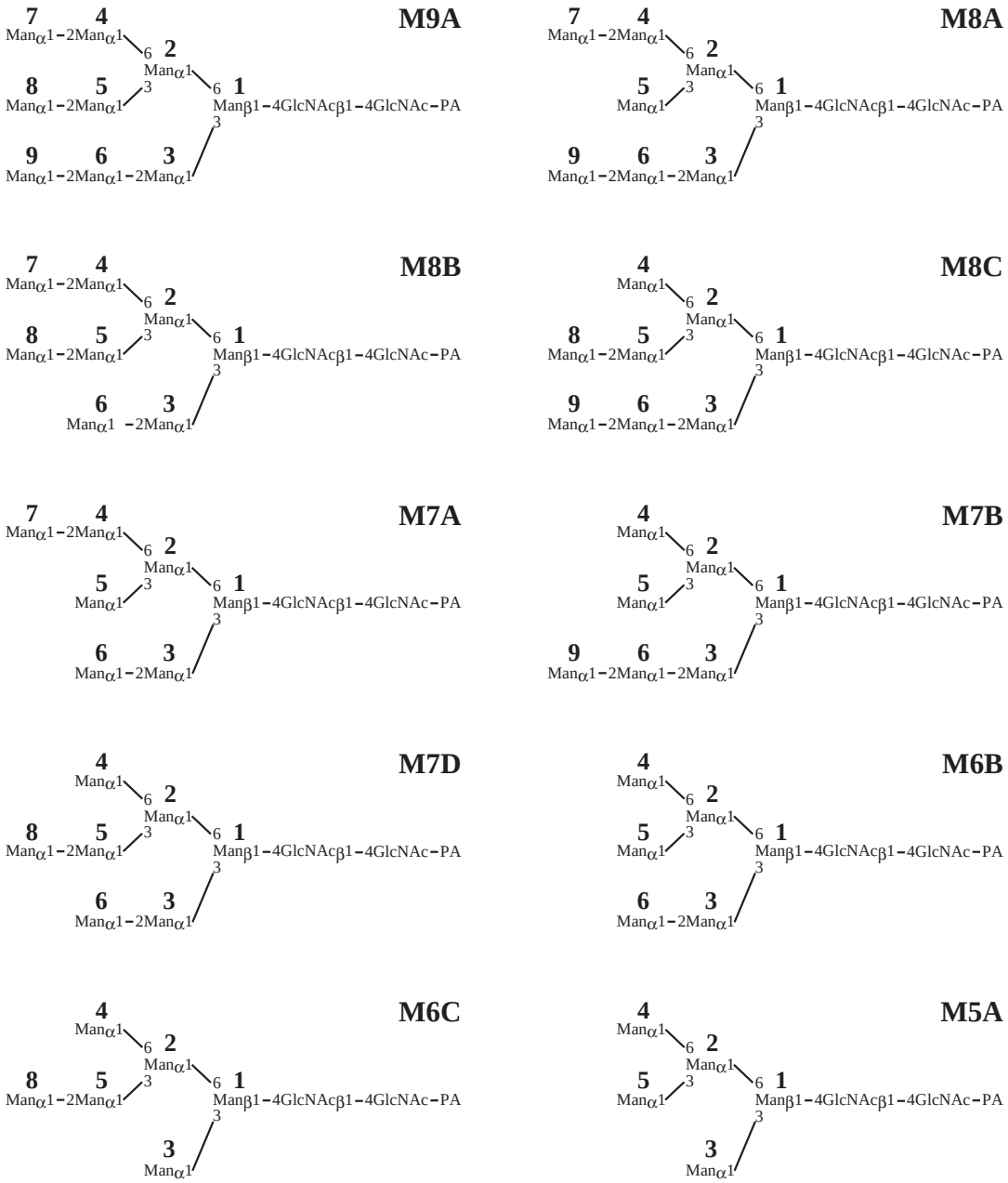

Figure 2. Structures of pyridylaminated oligosaccharides used as acceptors in this study. The position of each mannnose residue is numbered (**bold**).

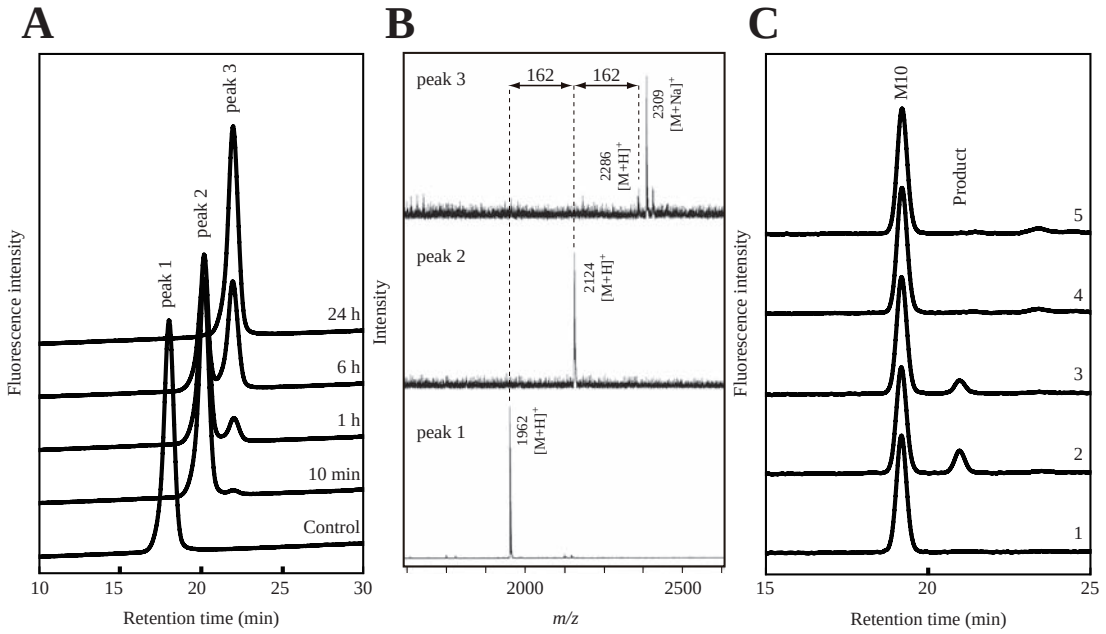

Figure 3. The novel product obtained from $Man_9GlcNAc_2$-PA by recombinant Och1p. ***A,*** $Man_9GlcNAc_2$-PA was incubated with 150 μg/ml Och1p for various periods indicated in the figure. The reaction mixtures were separated by HPLC by method 1 as described in Material and Methods. ***B,*** MALDI-TOF mass spectra of peaks 1, 2 and 3 in panel A. ***C,*** $Man_{10}GlcNAc_2$-PA produced by Och1p original activity was incubated with the concentrated supernatant containing wild-type Och1 or D187A mutant protein. The samples were separated by HPLC by method 3. Each chromatogram indicates as follows, 1; negative control ($Man_{10}GlcNAc_2$-PA), 2; after 24 h incubation with four-fold diluted crude enzyme containing wild-type Och1p, 3; after 24 h incubation with eight-fold diluted crude enzyme containing wild-type Och1p, 4; after 24 h incubation with crude enzyme containing D187A, 5; after 48 h incubation with crude enzyme containing D187A.

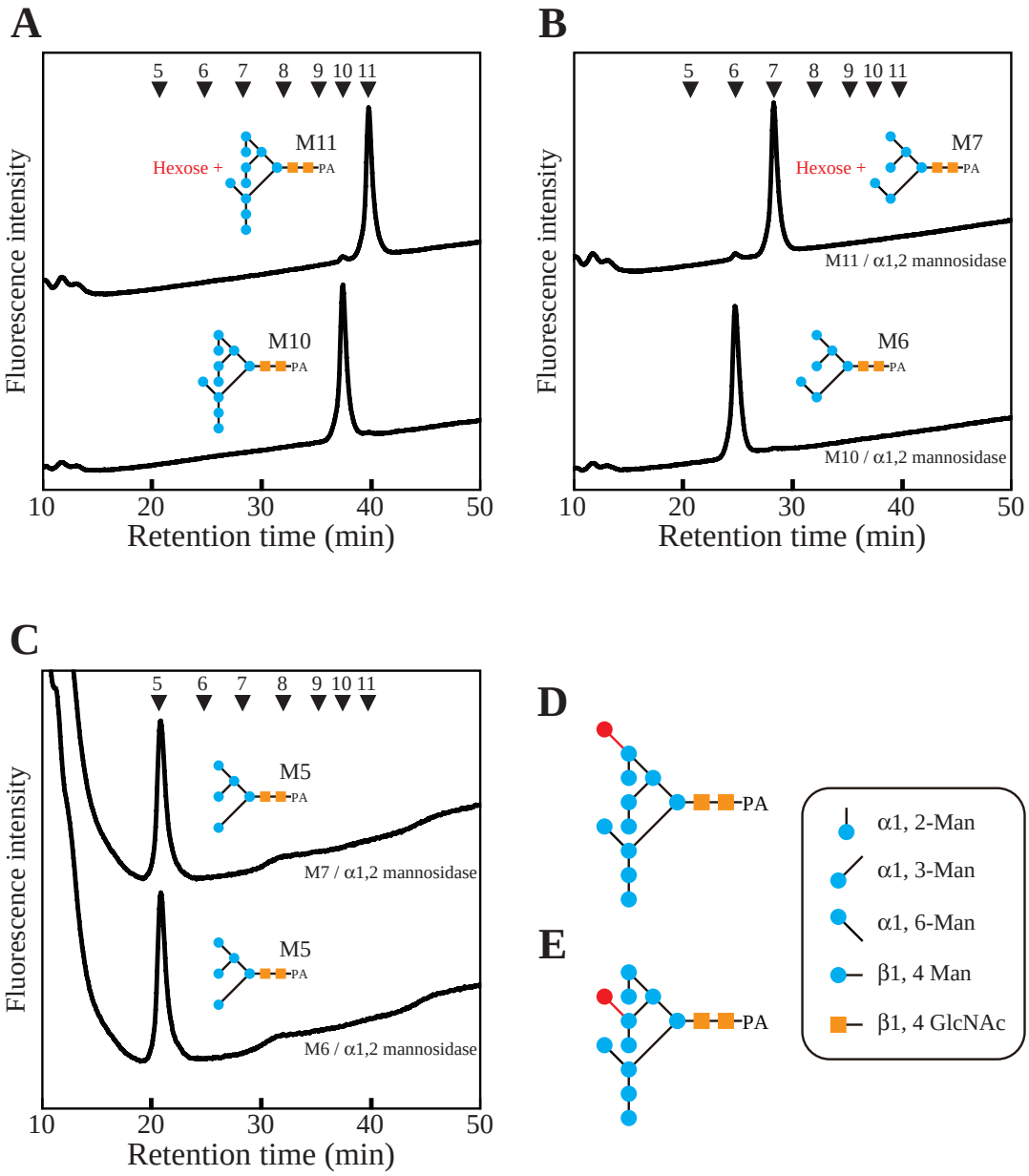

Figure 4. Confirmation of the structure of the novel product generated by recombinant Och1p. ***A,*** $Man_{10}GlcNAc_2$-PA (M10) and the novel product (M11) were analyzed by HPLC. ***B,*** after α1,2-mannosidase treatment of M11 and M10, the products were analyzed by HPLC. The $Man_7GlcNAc_2$-PA (M7) and $Man_6GlcNAc_2$-PA (M6) peaks were collected and subject to α1,6-mannosidase treatment. ***C,*** after α1,6-mannosidase treatment of M7 and M6, the products were analyzed by HPLC. These HPLC analyses were performed by method 1 as described in Materials and Methods. The numbers in the chromatograms indicate the mannose residue of each oligosaccharide. The predicted oligosaccharide structures are shown at the side of each peak. ***D and E,*** the schematic structures of M11 deduced from these results are shown. The red representaions are the additional α1,6-mannose residues transferred by Och1p.

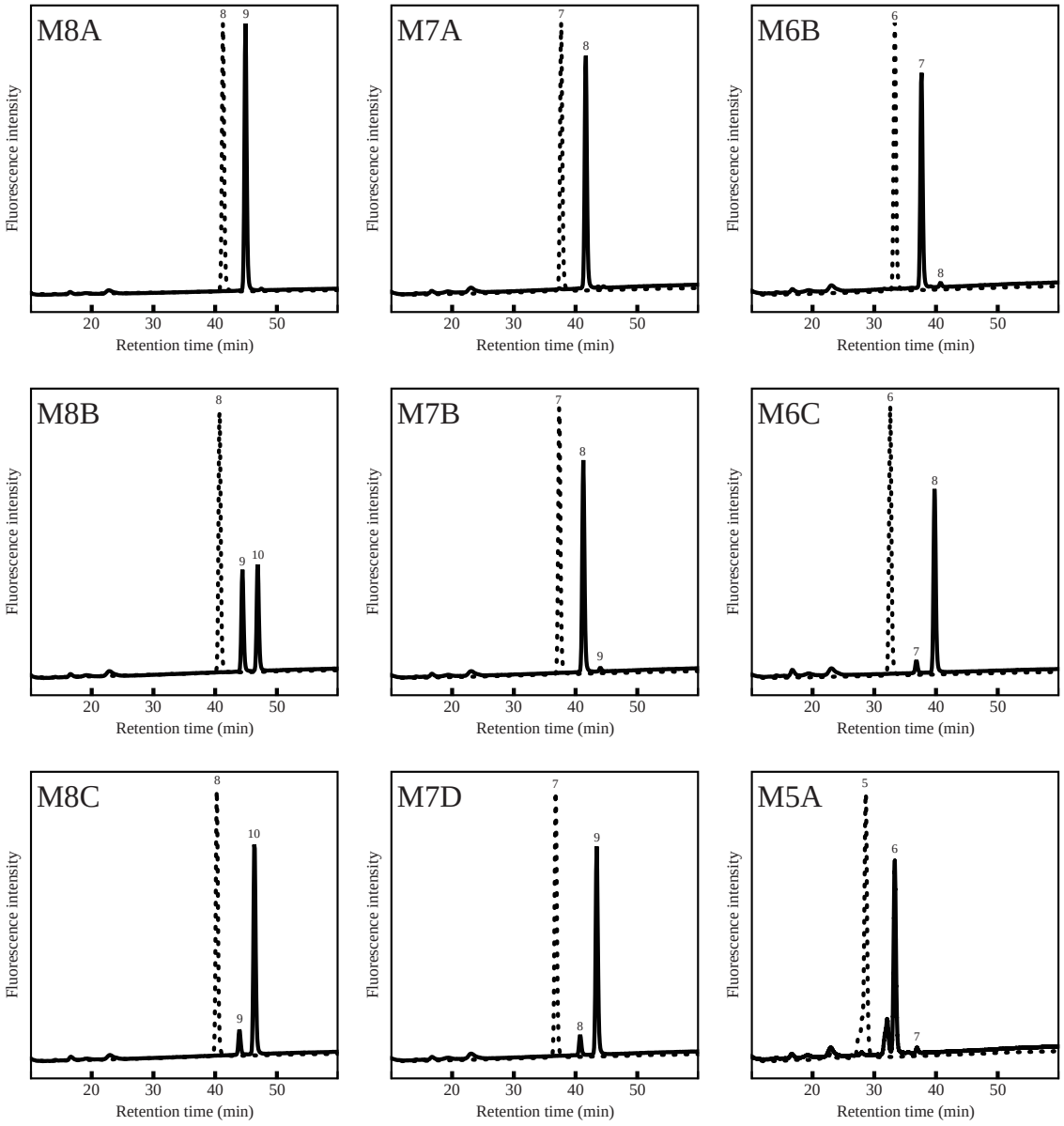

Figure 5. Effects of acceptor structure on the incorporation of an additional mannose by recombinant Och1p. Several acceptors were incubated with (solid lines) or without (dashed lines) 150 μg/ml Och1p. After enzymatic reaction for 6 h, the reaction mixtures were separated by HPLC by method 2 (Materials and Methods). The numbers of mannose residues are shown at the tops of peaks in each chromatogram.

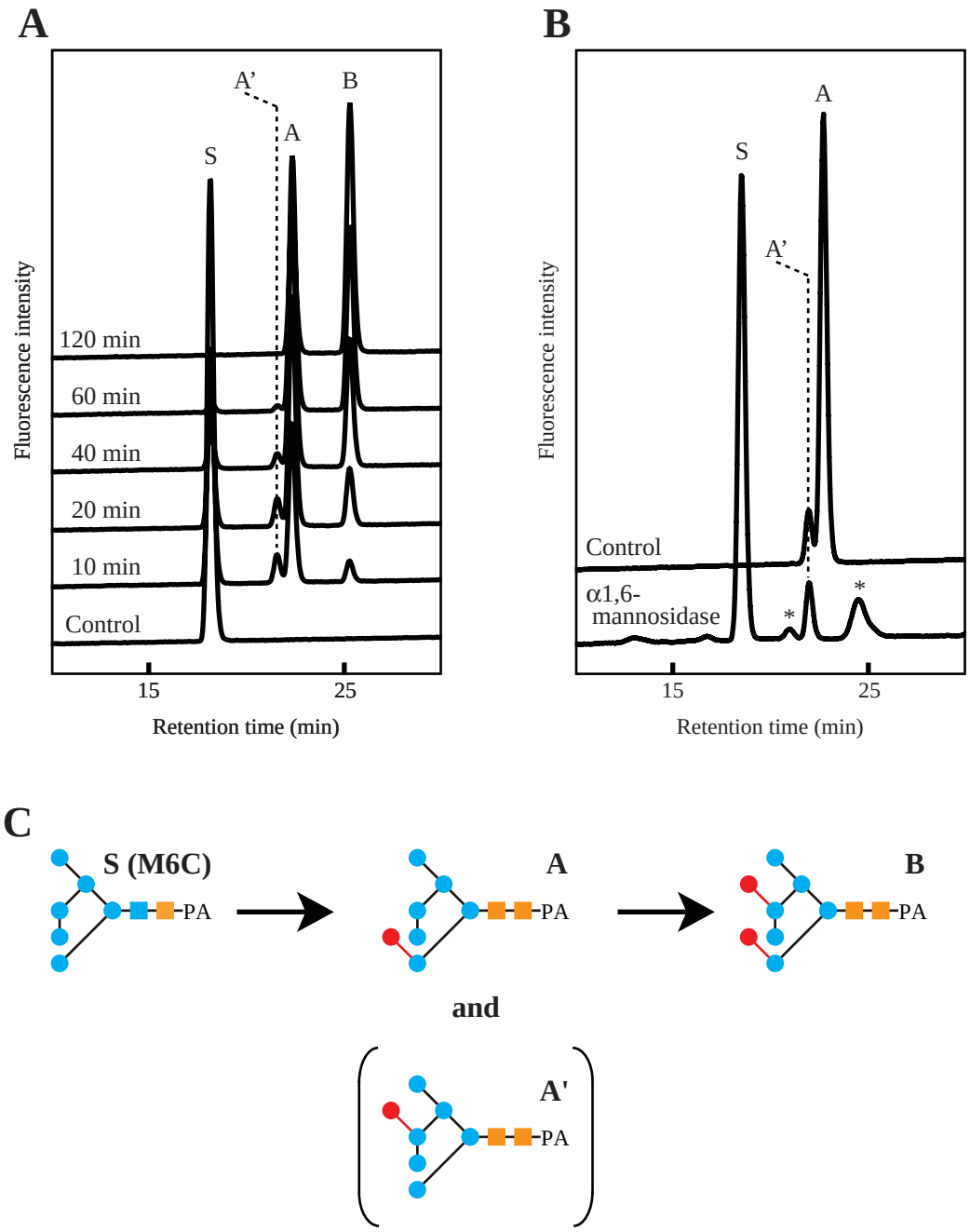

Figure 6. Positions of the first and second mannose additions to the M6C substrate. ***A,*** M6C (peak S) was incubated with 150 μg/ml Och1p for each indicated times. The reaction mixtures were separated by HPLC by method 2 (Materials and Methods). ***B,*** α1,6-mannosidase digestion of Och1p products containing peaks A' and A. The peaks marked with asterisks were contaminants derived from α1,6-mannosidase. ***C,*** process of synthesis of the novel products (A, A' and B) from M6C (S).

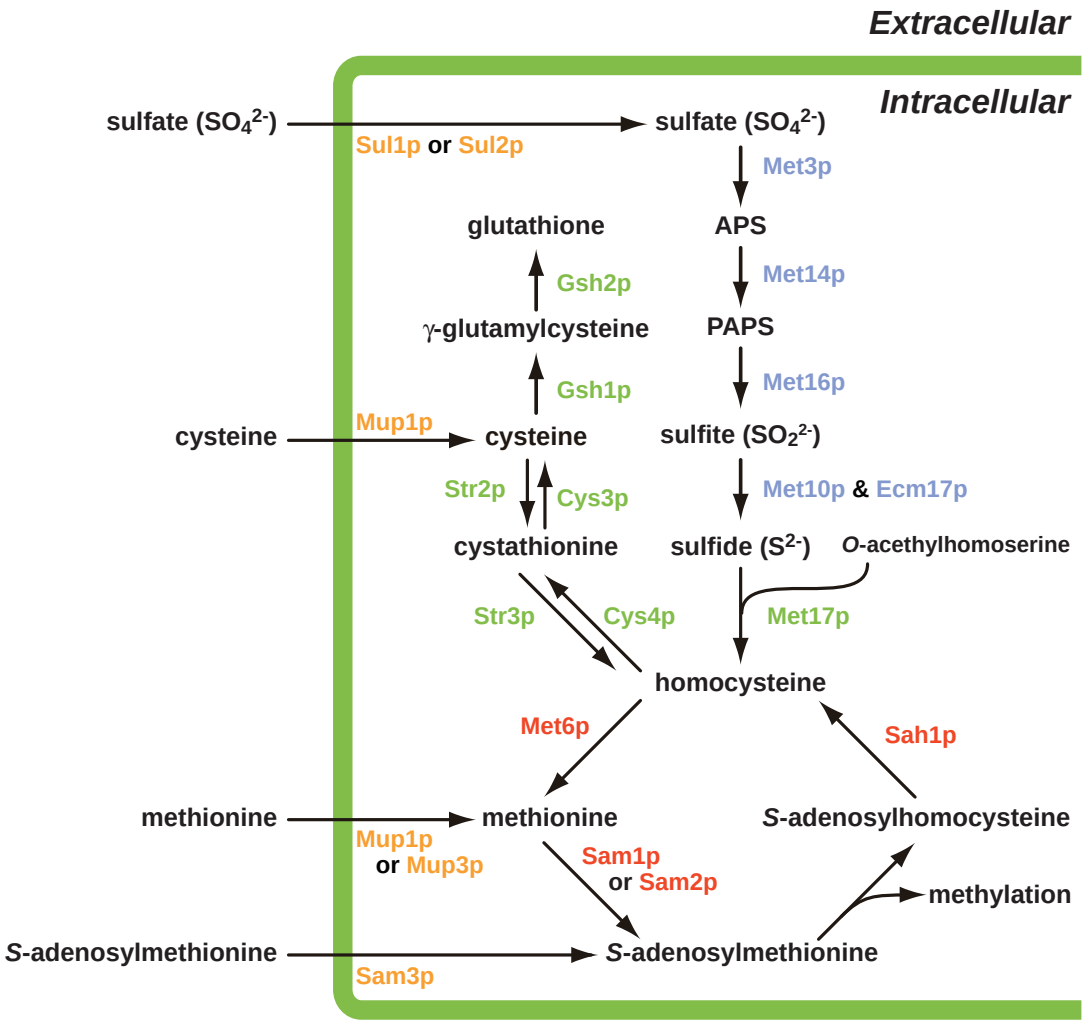

Figure7. Metabolic pathway of sulfur compounds in *S. cerevisiae*. The proteins involved in sulfur compounds uptake (orange), sulfate assimilation (blue), transsulfuration (green) and methyl cycle (red) are shown.

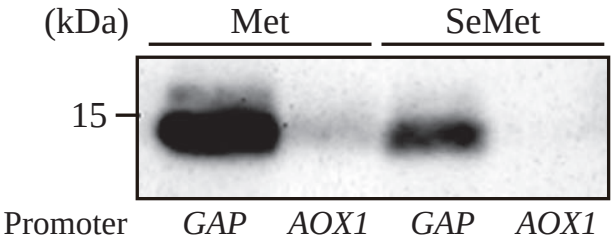

Figure 8. Comparison of productivity with promoters to produce recombinant HLY protein in synthetic complete medium. Each strain (SMD1168 background) was grown in BMGY for 24 h. The cells were washed with sterilized water, followed by resuspension in synthetic complete medium containing 100 μg/ml of methionine or SeMet. For strains that express HLY under the control of the *AOX1* promoter, methanol instead of glucose was used as a carbon source and was added every 24 h at a final concentration of 1%. After two days of cultivation in synthetic complete medium, the culture supernatants were analyzed by immunoblot (see Materials and Methods).

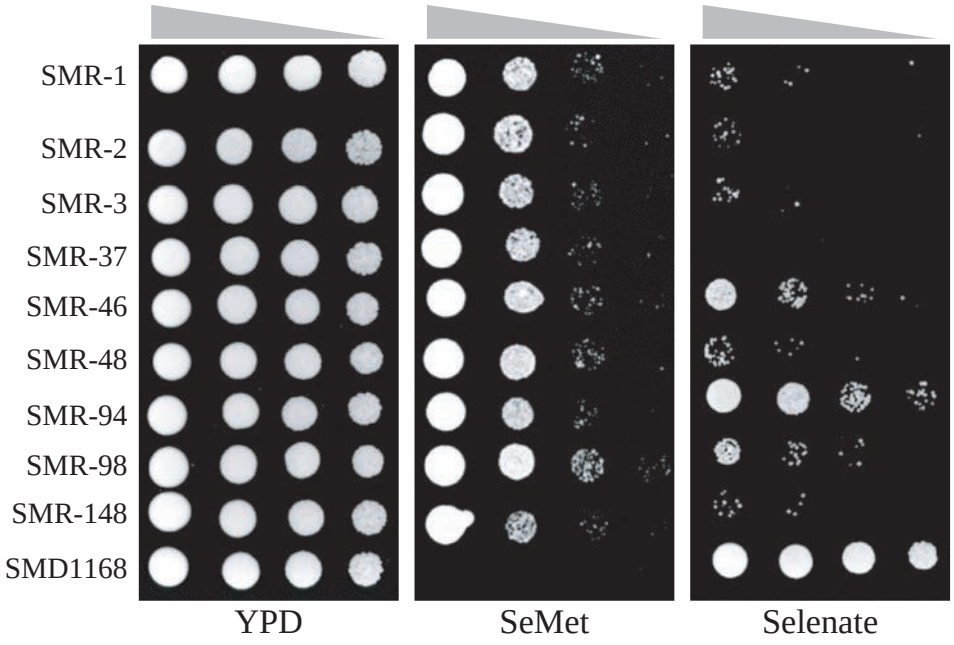

Figure 9. Growth phenotype of *P. pastoris* SMR mutants. Serial dilutions of SMR mutants were spotted on YPD, YPD containing 50 μg/ml of SeMet and YPD containing 10 mM selenate. The YPD plate and YPD plate containing selenate were incubated at 30˚C for two days, while the plate containing SeMet was incubated at 30˚C for three days.

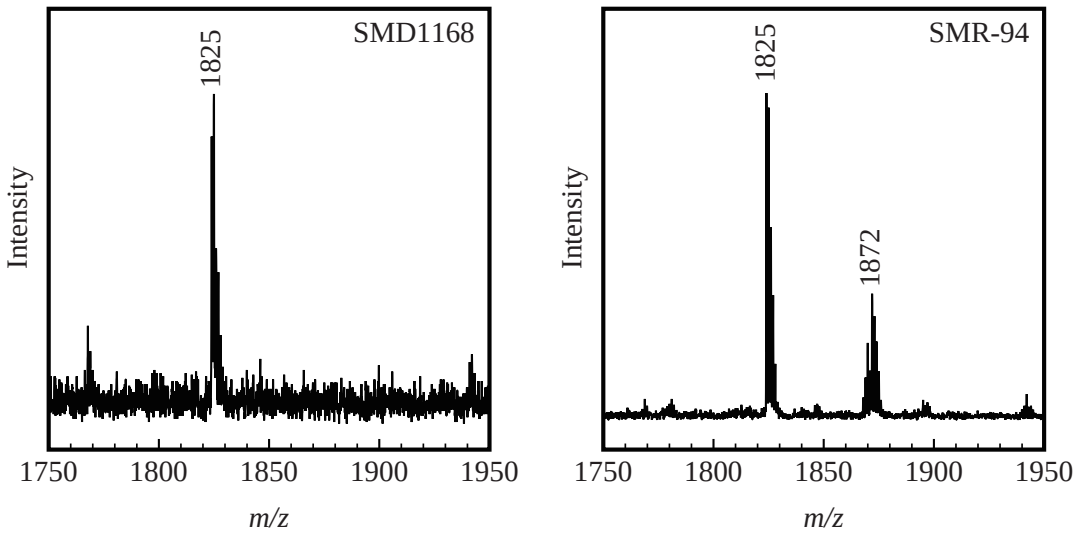

Figure 10. Peptide mass analyses of selenomethionyl HLY proteins. Purified HLY expressed by SMD1168 (50 μg/ml Met) or SMR-94 (50 μg/ml SeMet) was treated with trypsin, and subject to MALDI-TOF mass spectrometry. Because the trypsin digestions were performed without reducing agents, the prominent peak at *m/z* 1825 corresponds to the disulfide-bonded peptide that contains residues at both 22–33 (GISLANW**M**CLAK) and 116–119 (CQNR). Note that replacement of sulfur by selenium increases the mass value by 47.

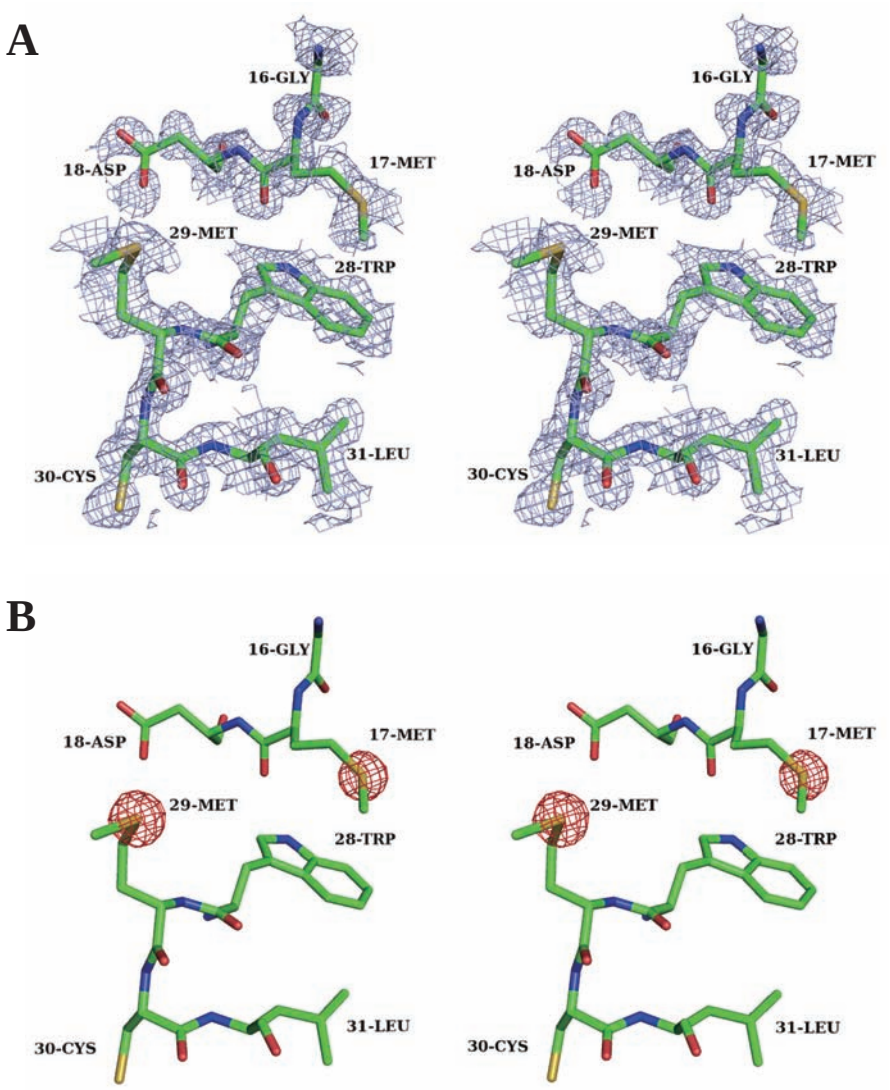

Figure 11. Stereoview of electron density maps in the region of 16-Gly, 17-Met, 18-Asp, 28-Trp, 29-Met, 30-Cys and 31-Leu. The refined HLY model (stick representation) is superimposed on the map (mesh representation). ***A,*** a SAD experimental electron density map contoured at 1.0σ was generated using the data from the DM program. ***B,*** an anomalous difference Fourier map contoured at 10σ, which was calculated using the phase from the Mlphare program. These figures were prepared with PyMOL.

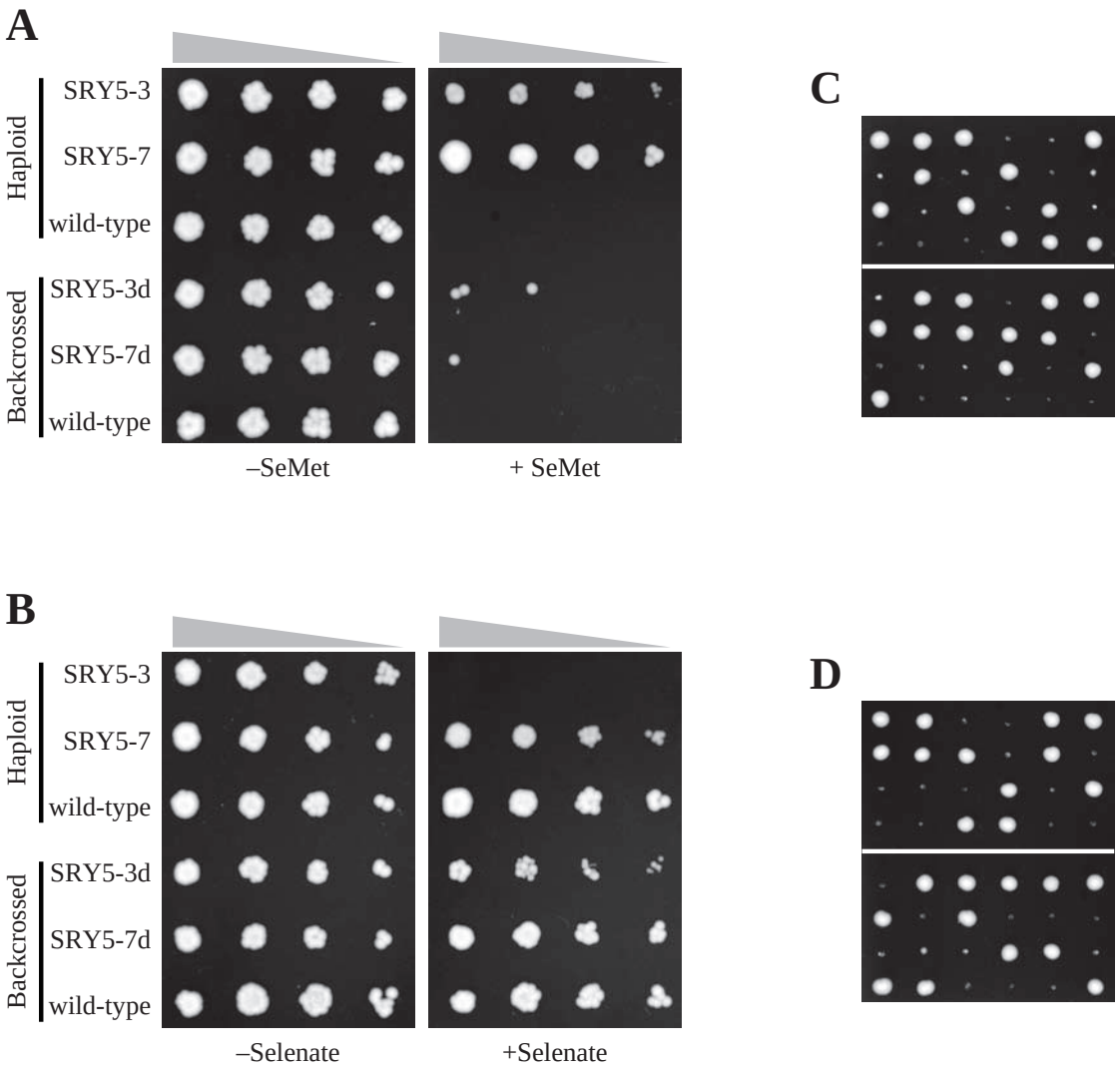

Figure 12. Growth phenotype of SeMet-resistant mutants. ***A,*** the haploid and the backcrossed mutants were incubated for three days at 30˚C on SD-Met medium supplemented with or without 10 μg/ml of SeMet. ***B,*** the haploid and the backcrossed mutants were incubated for two days at 30˚C on YPAD supplemented with or without 10 mM selenate. ***C and D,*** tetrads obtained from sporulation of SRY5-3d (panel C) or SRY5-7d (panel D) were incubated for three days at 30˚C on SD-Met medium containing 10 μg/ml of SeMet.

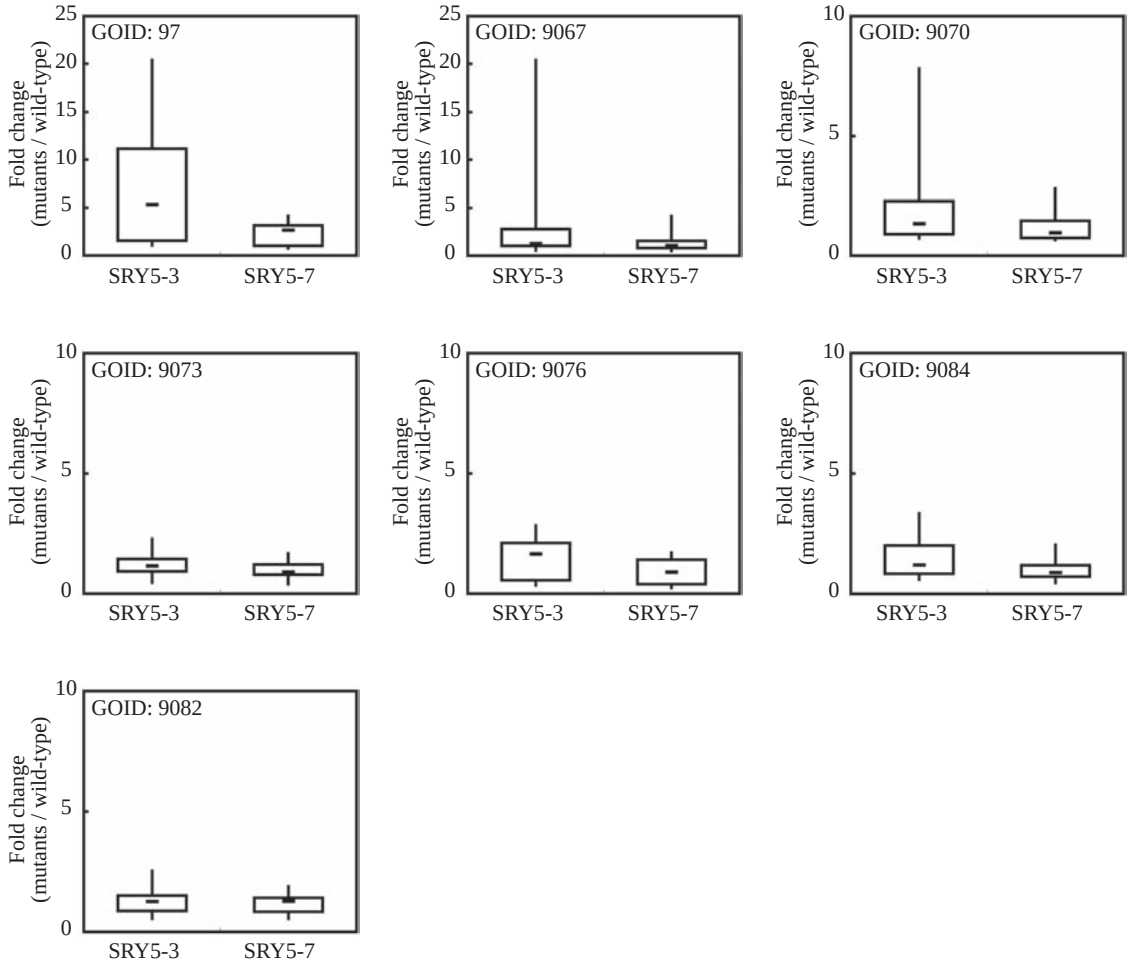

Figure13. Comparison gene expression level in each SeMet-resistant mutant. Boxplots of expression profile of the genes involved in sulfur amino acid biosynthetic process (GOID: 97), asparatate family amino acid biosynthetic process (GOID: 9067), serine family amino acid biosynthetic process (GOID: 9070), aromatic amino acid family biosynthetic process (GOID: 9073), histidine family amino acid biosynthetic process (GOID: 9076), branched chain family amino acid biosynthetic process (GOID: 9082) and glutamine family amino acid biosynthetic process (GOID: 9084) are shown.

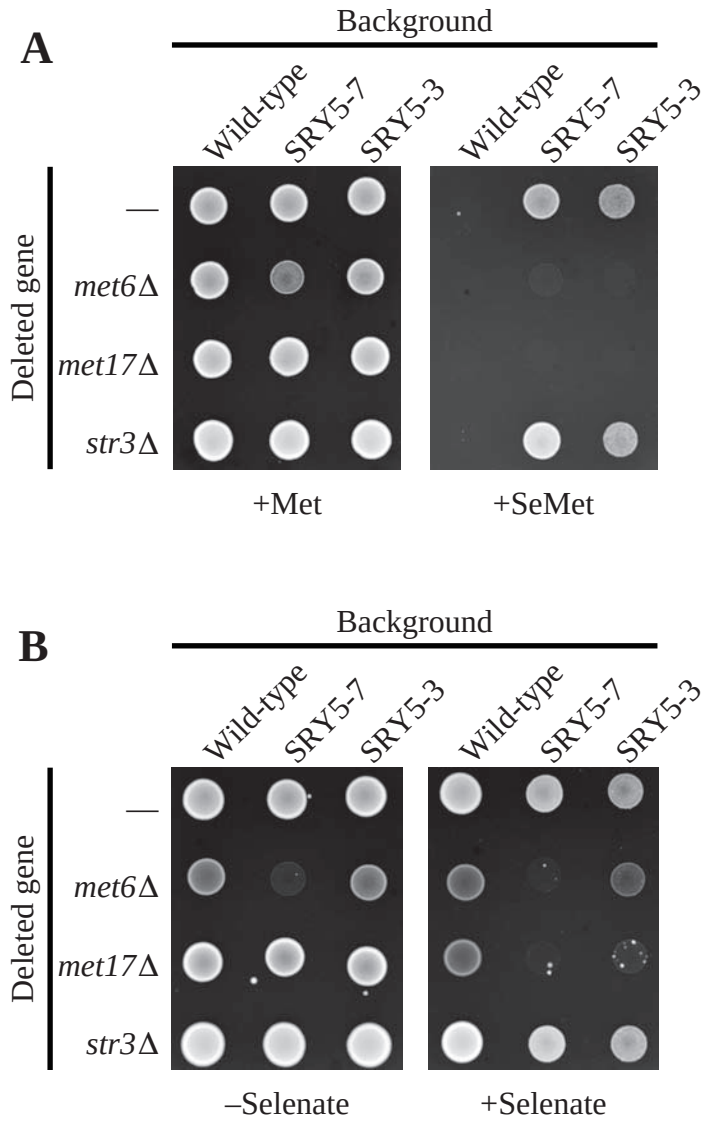

Figure 14. Alteration of phenotypes of SeMet-resistant mutants by the blocking of methionine synthesis. *A,* SeMet-resistant mutants completely laking the ORF of *MET6*, *MET17* or *STR3* were spotted on SD medium containing 20 μg/ml of methionine or 10 μg/ml of SeMet instead of methionine. The parental strains were also spotted as controls. The plates incubated for two days at 30˚C. ***B,*** the above mentioned strains were incubated on SD medium, which contained 5 μg/ml of methionine, supplemented with or without 10 mM selenate for two days at 30˚C.

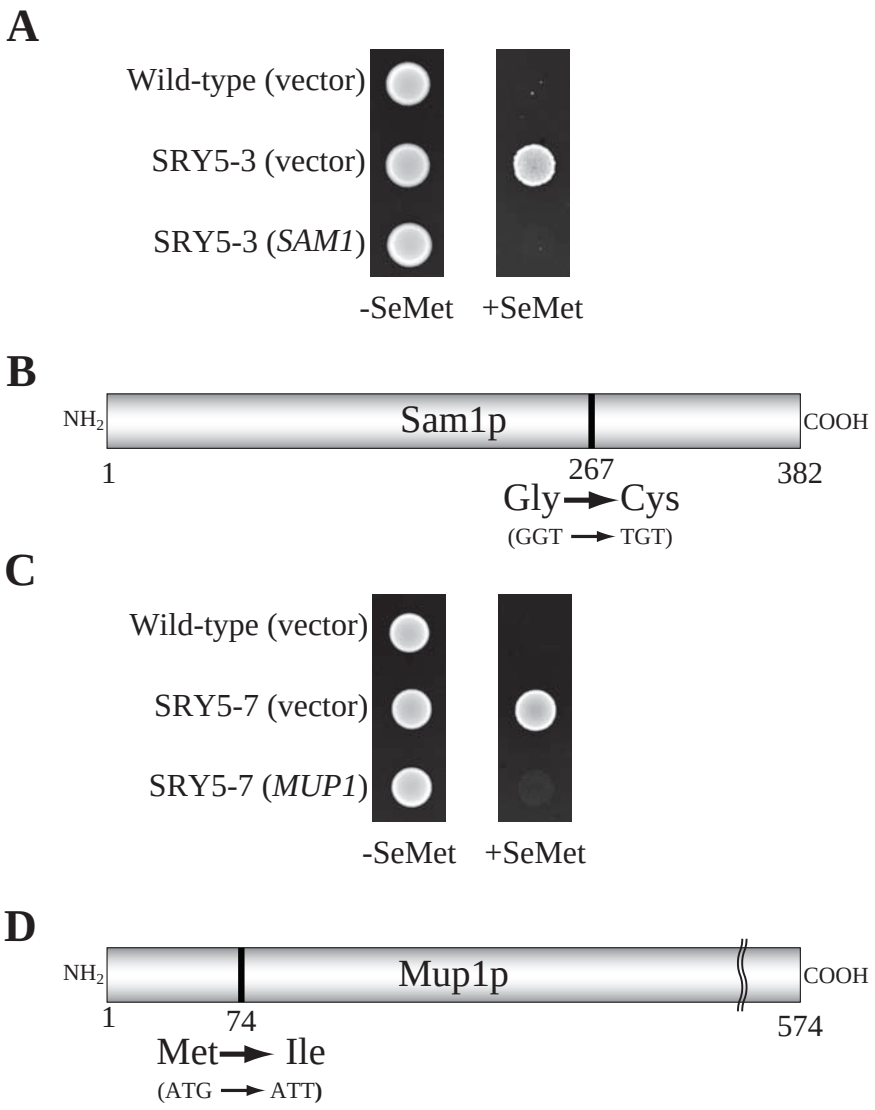

Figure15. Complementation of SeMet-resistant mutants. ***A,*** SRY5-3 was transformed with a centromeric plasmid (*URA3* marker) containing *SAM1* gene (*SAM1*). Wild-type and SRY5-3 were also transformed with the plasmid backbone (vector) as controls. The transformants were incubated on the SD medium, which lacked uracil and methionine, supplemented with or without 10 μg/ml of SeMet for three days at 30˚C. ***B,*** schematic representation of mutant protein encoded by *sam1-224*. The relative position of mutation changing the codon glycine to cysteine is indicated. ***C,*** SRY5-7 was transformed with a centromeric plasmid (*URA3* marker) containing *MUP1* gene (*MUP1*). Wild-type and SRY5-7 were also transformed with the plasmid backbone (vector) as controls. The transformants were incubated under the same condition in panel A. ***D,*** schematic representation of mutant protein encoded by *mup1-100*. The relative position of mutation changing the codon methionine to isoleucine is indicated.

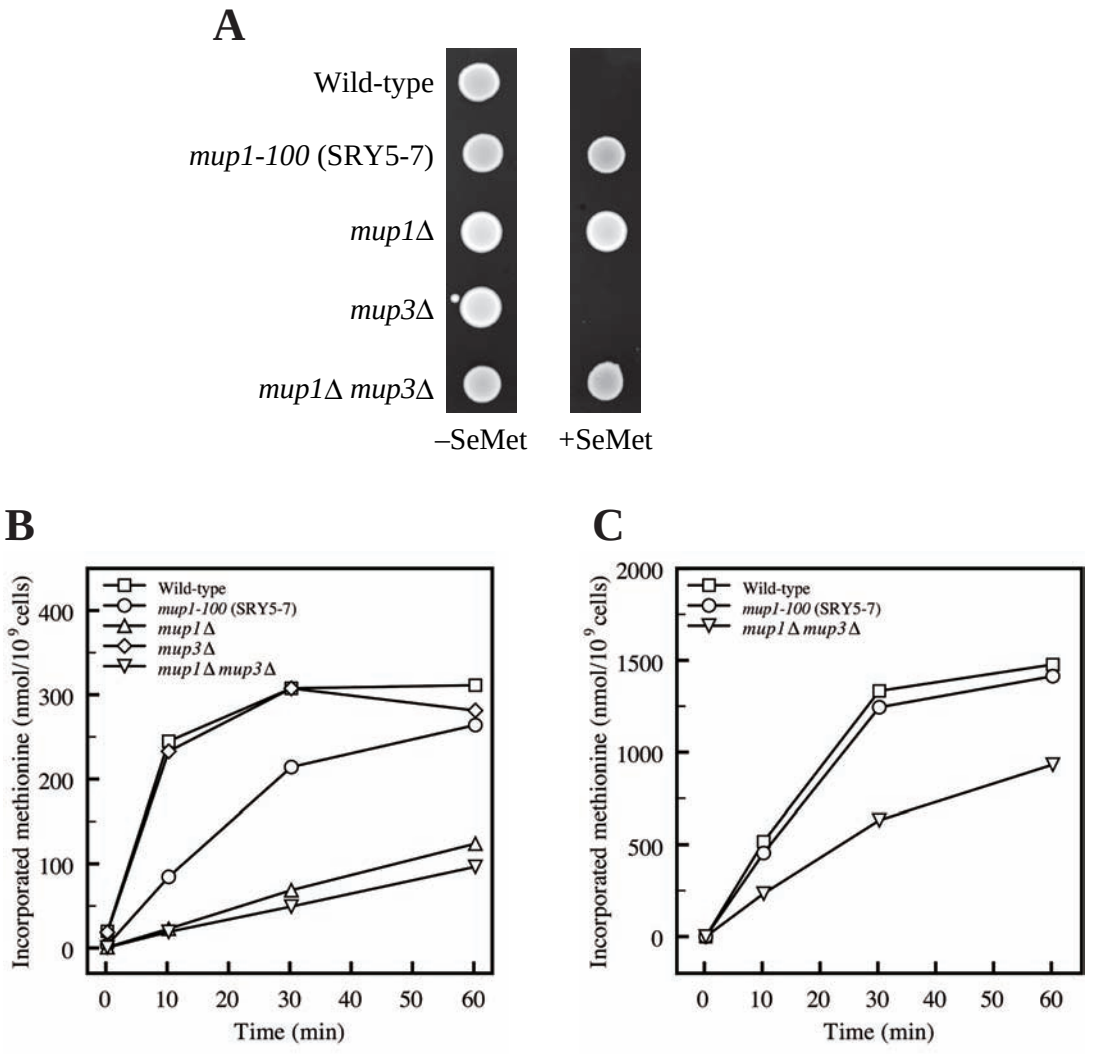

Figure 16. Effect of the mutation of genes encoding methionine permease on SeMet resistance and methionine uptake. ***A,*** the indicated strains were incubated on SD-Met medium suplemented with or without 10 μg/ml of SeMet for two days at 30˚C. ***B and C,*** cells were grown to mid-logarithmic phase at 30˚C in minimal medium containing amino acids and bases needed to meet their auxotrophic requirements. Uptake was started by the adding of methionine solution containing 30.2 kBq of [methyl-^{3}H] methionine at a final concentration of 20 μM (panel B) and 250 μM (panel C), and mesured at the indicated time points. The amount of incorporated mthionine was normalized by the number of cells, which was determined from A_{600} (1.0 A_{600} = 1.0×10^7 cells). Assays were performed in duplicate.